Development of the Composite YOY Index for Bluefish

Katie Drew

September 2022

Introduction

States from New Hampshire to Virginia conduct seine surveys for juvenile finfish that capture young-of-year bluefish. These surveys are noisy and cover small geographical areas, compared to the range of bluefish. Bayesian hierarchical modeling was used to combine these indices into a single composite index, using the method developed by Conn (2010), to represent the recruitment dynamics of bluefish on a larger scale.

Methods

Surveys included in the base model run of the composite index were:

- New Hampshire Juvenile Finfish Seine Survey
- Rhode Island Narragansett Bay Juvenile Finfish Beach Seine Survey
- New York Western Long Island Seine Survey
- New Jersey Delaware River Seine Survey
- Maryland Chesapeake Bay Juvenile Striped Bass Seine Survey
- Virginia Chesapeake Bay Juvenile Striped Bass Seine Survey

All surveys were fixed station seine surveys; indices were calculated as the geometric mean catch-per-haul with CVs calculated using a bootstrap approach. For a complete description of the survey methods, see the ASMFC State Data Review Workshop Report (ASMFC 2021).

The Conn (2010) method assumes that all indices are tracking the abundance of recruits, but are also influenced by sampling error and process error (e.g., sampling different components of the coastwide recruit population).

$$\log(U_t) \sim Normal(\log(\mu_t) + \log(q_{it}), \left(\sigma_{it}^{p}\right)^2 + \left(\sigma_{it}^{S}\right)^2)$$

A Bayesian analysis was performed to estimate the true trend in relative abundance of recruits as well as the process error and catchability associated with each survey. The input parameters and priors were chosen to be the same as Conn (2010) and the Atlantic Menhaden assessment (SEDAR 2015) used.

A Normal(log(100), 1) distribution was chosen for $\nu_t = \log(\mu_t)$ The mean of this distribution, log(100), was chosen so that the mean of the relative abundance time series would be approximately 100. This number is arbitrary, since we are interested in the trends in relative abundance, not the actual number.

For catchability, which is assumed constant for each survey and estimated in log-space, $\chi_i = \log(q_i)$ was set as χ_i = Normal(log(0.01), 0.5).

For process error (σ^p), Gelman (2006) suggests that a Uniform(0,m) distribution may perform better than other choices when there is a small number of group effects. A Uniform(0, 5) prior distribution for σ^p, which gives equal weight to all plausible precision values, was specified. Process error was assumed constant over time but estimated for each survey.

The observed CVs from the surveys were used as the input sampling error (σ^S). Several surveys had years with zero bluefish catch; those zeros were replaced with the smallest value in the time series divided by 1,000 to retain the information that the survey had occurred and the abundance was extremely low in that year rather than treat them as missing data. The largest CV in the time series, multiplied by 150%, was used as the CV for those observations.

All posterior simulation was performed using the software package OpenBUGS (Lunn et al. 2009), with the package R2OpenBUGS (Sturtz et al. 2005). Standard Bayesian diagnostics, including trace plots and autocorrelation plots, were used to assess convergence and stability of results.

As a sensitivity run, a composite index was also developed using the GLM-standardized YOY indices (see Working Paper 7 Celestino et al. 2022a) and using a set of trawl YOY indices collected in similar geographic areas (ASMFC 2021). The composite indices were compared to the SEAMAP age-0 and age-1 indices, which covered the southern end of the bluefish range, as well as the age-specific components of the age-0+ fishery-independent indices and the age-0 total catch to examine consistency among the input datasets.

Results

The diagnostic plots indicated acceptable performance of the Bayesian fitting routine (Appendix 1 of this working paper).

The composite index tracked several consistently strong recruitment events that were registered by multiple surveys, and smoothed out the noise somewhat in years with weaker signals (Figure 1). The base model of the composite index did not show a strong trend over time; it was higher at the beginning of the time series than at the end, but the uncertainty around the index at the beginning of the time series was also higher (Table 1, Figure 2). Using the standardized indices and the trawl indices produced composite indices that were similar in trend and generally within the confidence intervals of the base model (Figure 3).

The base model composite index was moderately correlated with the age-0 catch (Figure 4) and the age-0 component of the NC PSIGN survey (Figure 5), as well as the lagged age-2 component of the ChesMMAP index (Figure 6). It was not correlated with the SEAMAP age-0 or lagged age-1 indices (Figure 7), or with any ages of the other surveys (Figure 8 - Figure 10). This may be related to the areas covered by these surveys: the seine surveys in the composite index occur in estuaries and tidal rivers. ChesMMAP and NC PSIGNS are conducted in inshore bays and estuaries while SEAMAP, NEAMAP, and the NEFSC bottom trawl surveys occur in ocean waters further offshore. Supporting this hypothesis is the fact that the SEAMAP age-0 was more strongly correlated with the age-0 and lagged age-1 components of the NEFSC Albatross index and lagged older ages of the NEAMAP survey than the composite index was (Figure 11and Figure 12).

The composite indices developed from trawl YOY surveys and from the standardized seine indices were not well correlated with the age-0 catch or any of the other indices. The lack of consistency with other data sources supported the decision to use the seine indices in the base model of the composite YOY index.

Literature Cited

ASMFC. 2021. Report from the 2021 Bluefish State Data Review Workshop. Arlington, VA. 115p. Available online at: https://www.asmfc.org/uploads/file/63487cfe2021BluefishStateDataReviewReport.pdf

Conn, P. B. 2010. Hierarchical analysis of multiple noisy abundance indices. Canadian Journal of Fisheries and Aquatic Sciences 67(1): 108-120.

Gelman, A. 2006. Prior distributions for variance parameters in hierarchical models (comment on article by Browne and Draper). Bayesian Anal. 3: 515–534.

Lunn, D., Spiegelhalter, D., Thomas, A. and Best, N. 2009. The BUGS project: Evolution, critique and future directions. Statist. Med., 28: 3049-3067. https://doi.org/10.1002/sim.3680

SEDAR. 2015. SEDAR 40 – Atlantic Menhaden Stock Assessment Report. SEDAR, North Charleston SC. 643 pp. available online at: http://www.asmfc.org/uploads/file/55089931S40_AtlMenhadenSAR_CombinedFINAL_1.15.2015-reduced.pdf

Sturtz, S., Ligges, U., and Gelman, A. 2005. R2WinBUGS: a package for running WinBUGS from R. J. Stat. Softw. 12: 1–16.

Tables

Table 1. Composite YOY index and CV

Year	CPUE	CV
1981	0.690	1.050
1982	2.153	0.980
1983	1.022	1.028
1984	0.843	1.034
1985	2.158	1.002
1986	1.171	1.010
1987	1.552	0.540
1988	1.069	0.381
1989	1.612	0.383
1990	1.301	0.365
1991	1.743	0.360
1992	0.631	0.421
1993	0.492	0.384
1994	0.635	0.390
1995	0.561	0.377
1996	0.928	0.368
1997	1.413	0.361
1998	0.768	0.393
1999	1.633	0.472
2000	0.601	0.378
2001	1.448	0.370
2002	0.649	0.288
2003	0.634	0.302
2004	0.714	0.294
2005	1.450	0.289
2006	0.994	0.283
2007	0.950	0.299
2008	1.057	0.289
2009	0.821	0.305
2010	0.956	0.285
2011	0.801	0.299
2012	0.727	0.306
2013	1.154	0.272
2014	1.265	0.273
2015	0.586	0.292
2016	0.467	0.319
2017	0.706	0.322
2018	0.401	0.348
2019	0.665	0.320
2020	0.785	0.366
2021	0.795	0.336

Figures

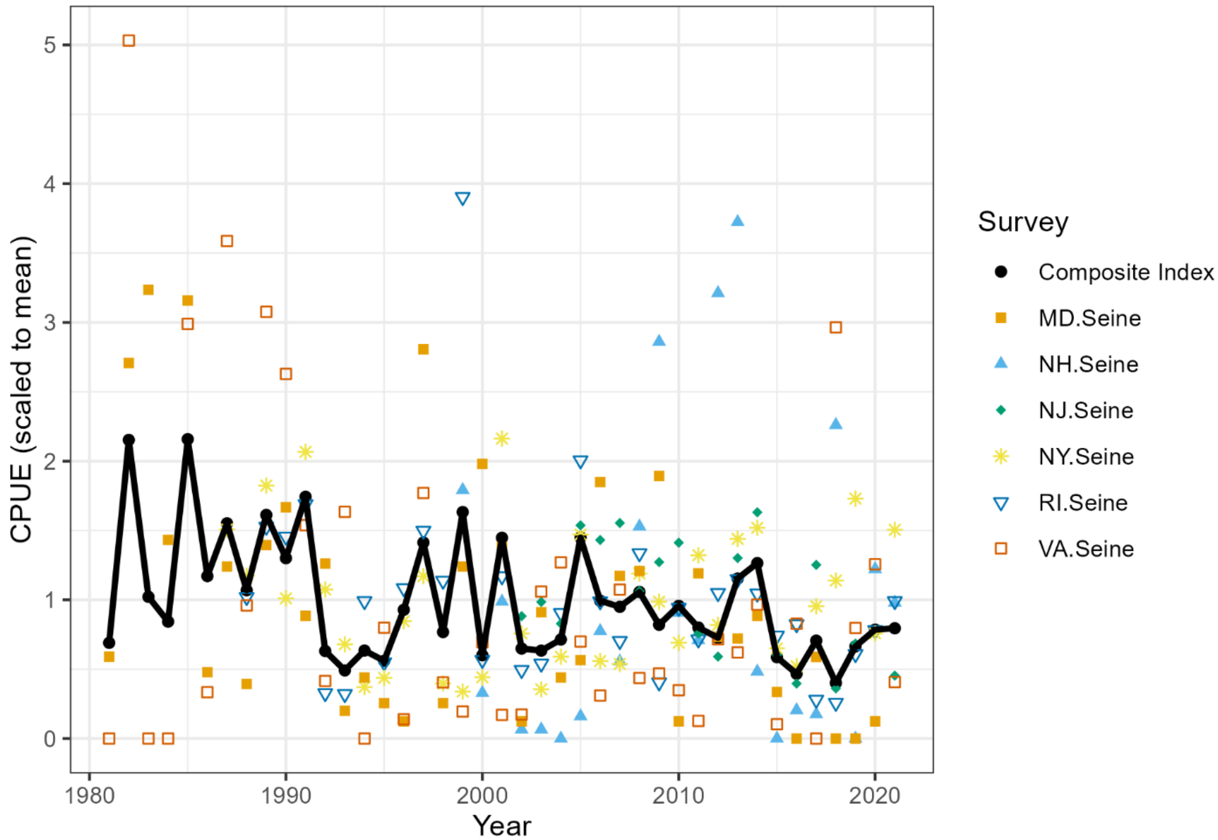

Figure 1. Composite YOY index plotted with individual seine surveys used as input.

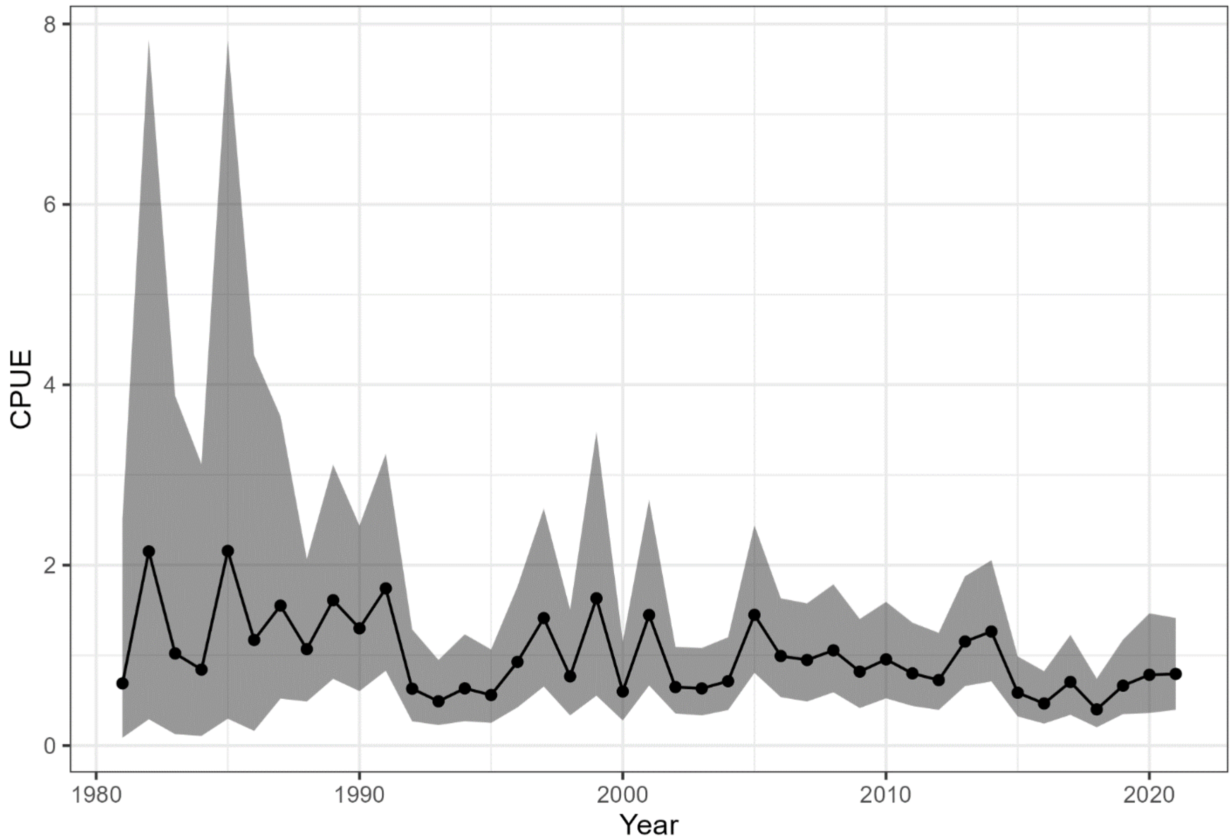

Figure 2. Composite YOY index plotted with 95% confidence intervals.

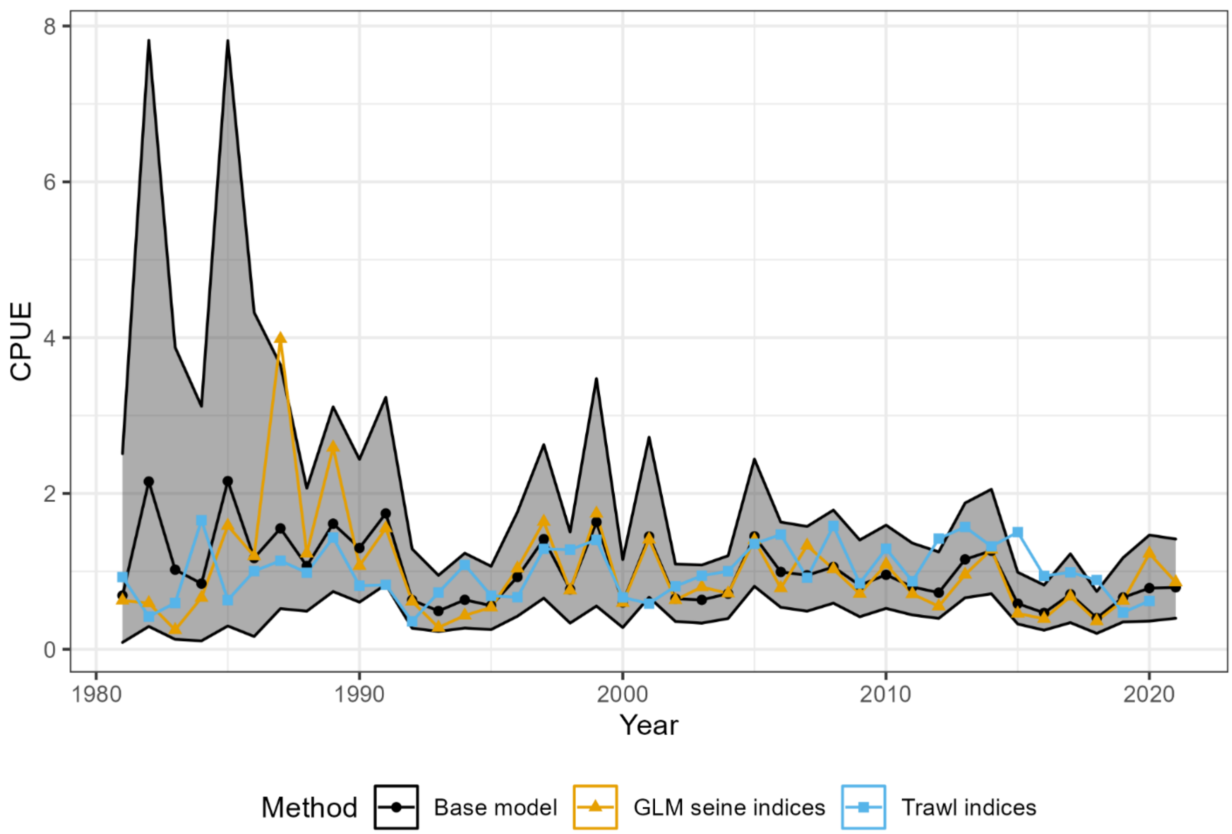

Figure 3. The base model composite YOY index plotted with the composite index developed using the GLM-standardized seine indices and the composite index developed with trawl YOY indices. The shaded area indicates the 95% confidence intervals of the base model.

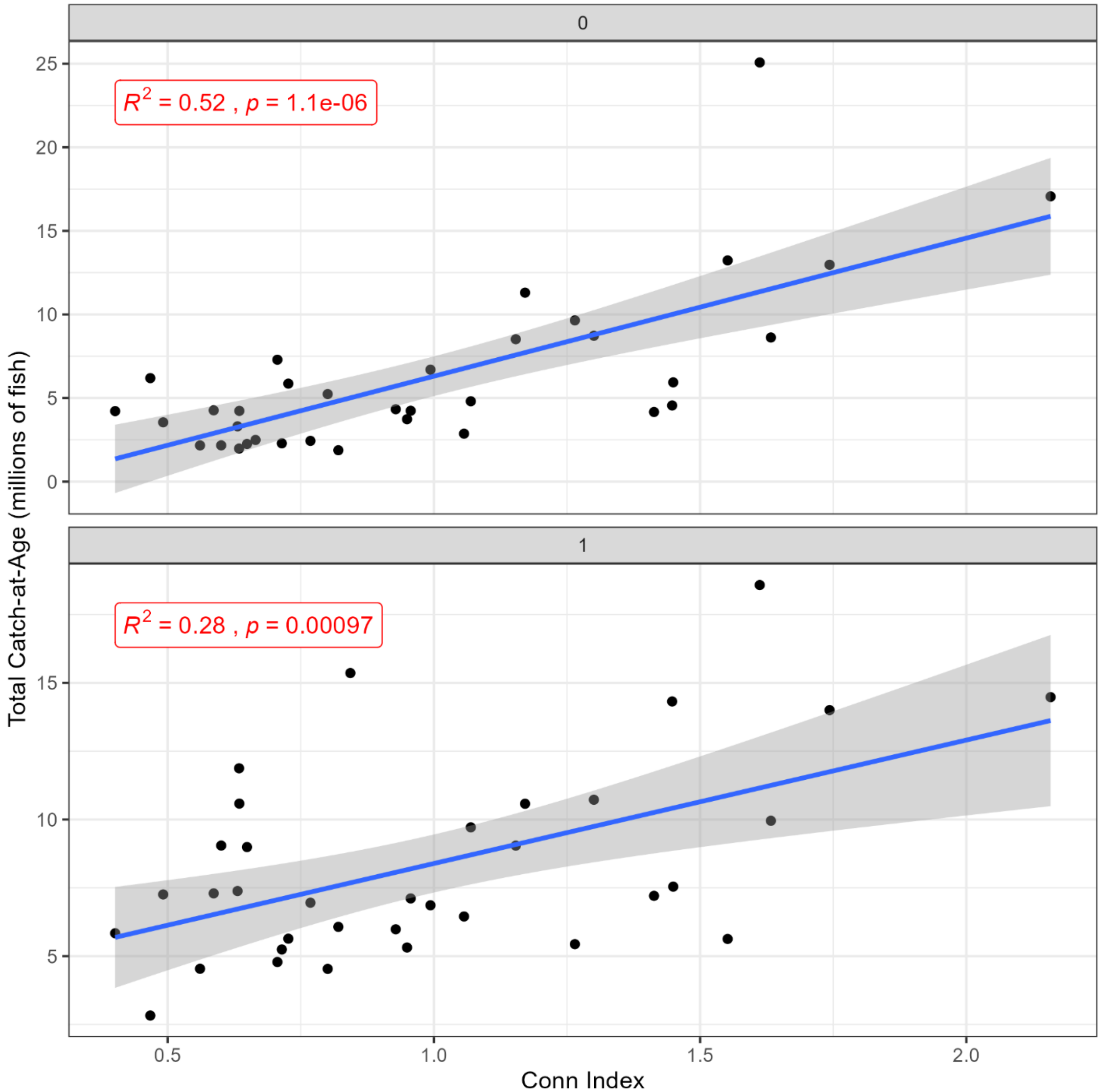

Figure 4. Total catch-at-age for age-0 (top) and age-1 (bottom) plotted against the composite YOY index.

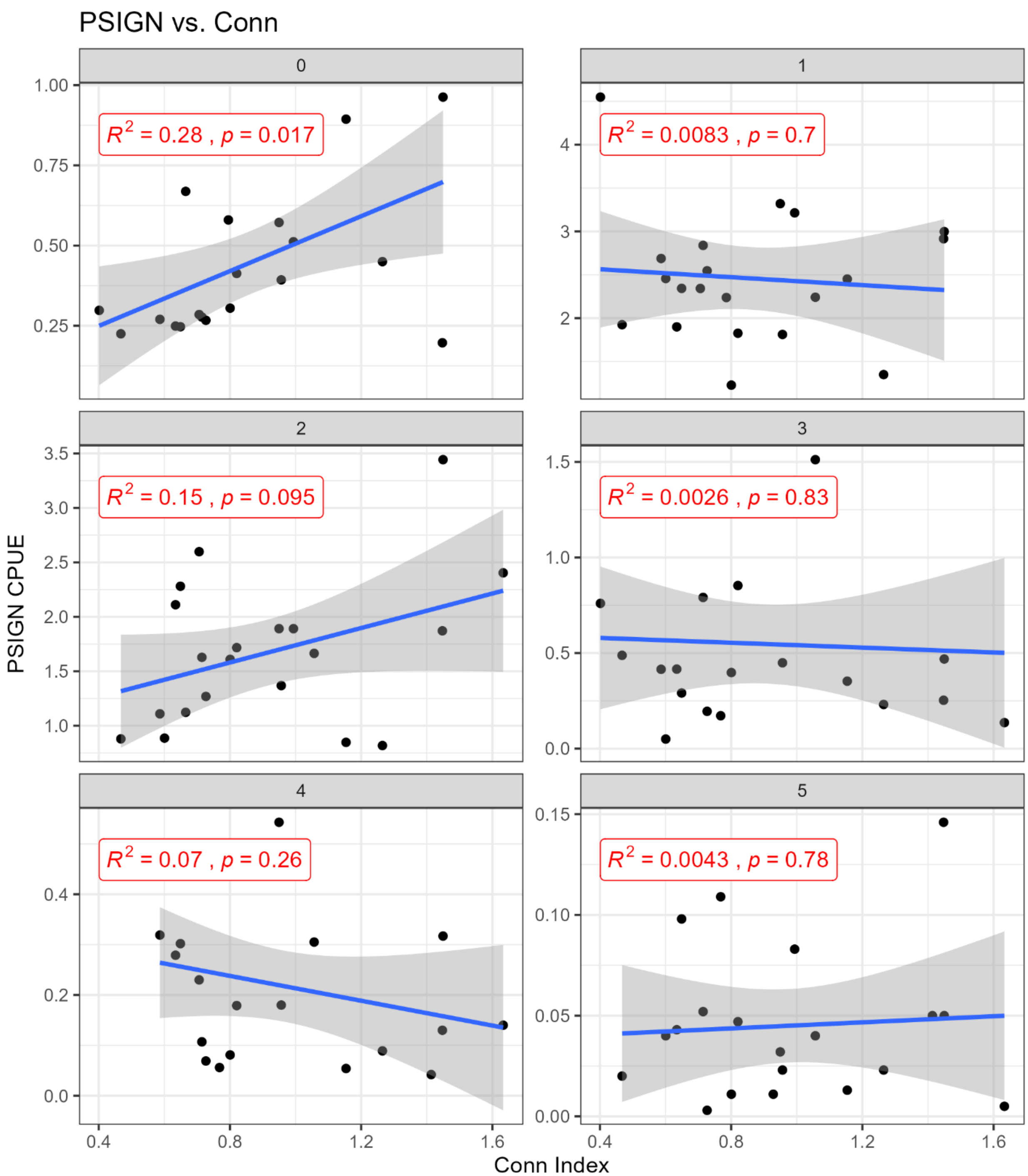

Figure 5. NC PSIGN index-at-age plotted against the composite YOY index.

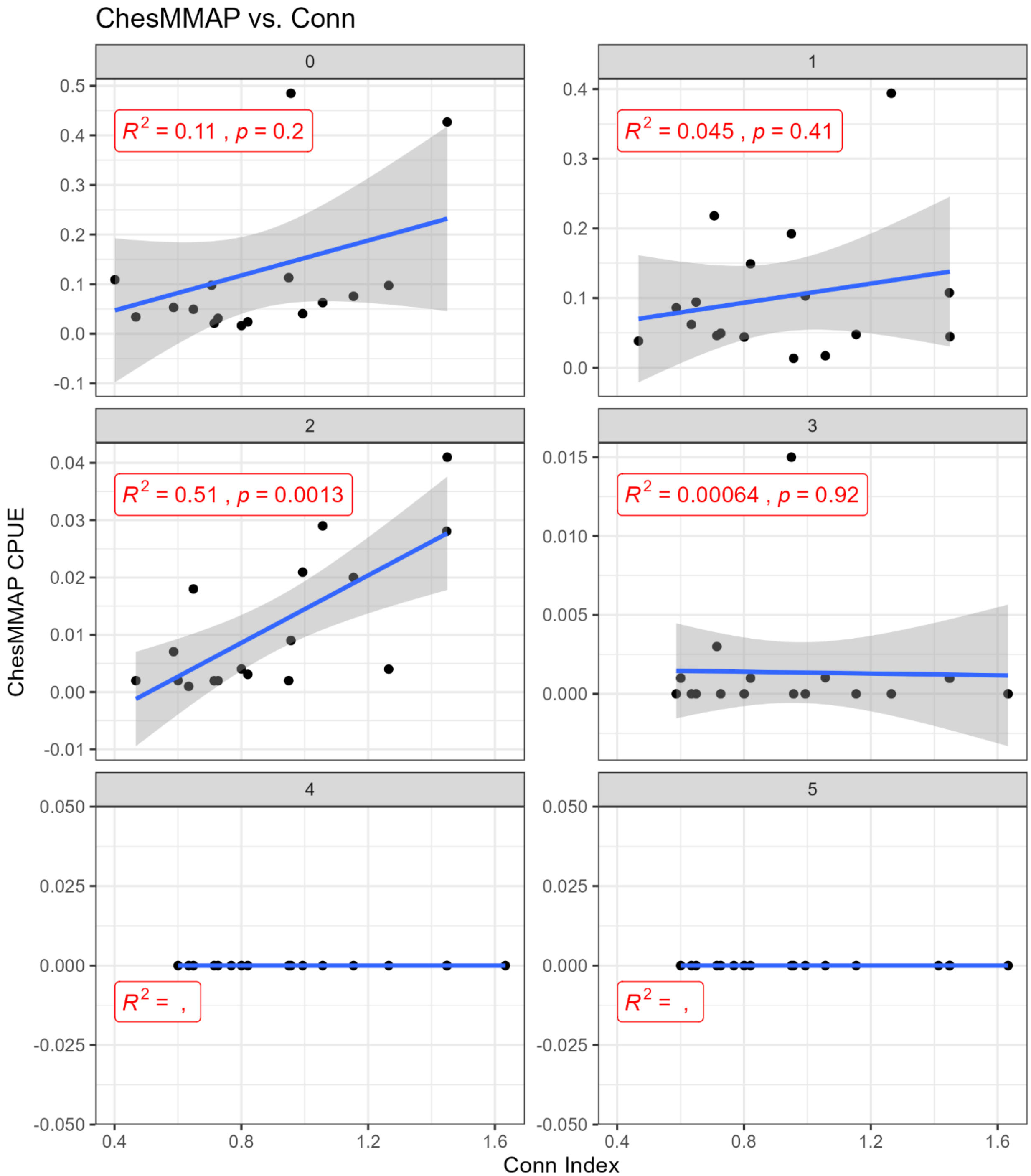

Figure 6. ChesMMAP index-at-age plotted against the composite YOY index. ChesMMAP does not catch ages greater than 3.

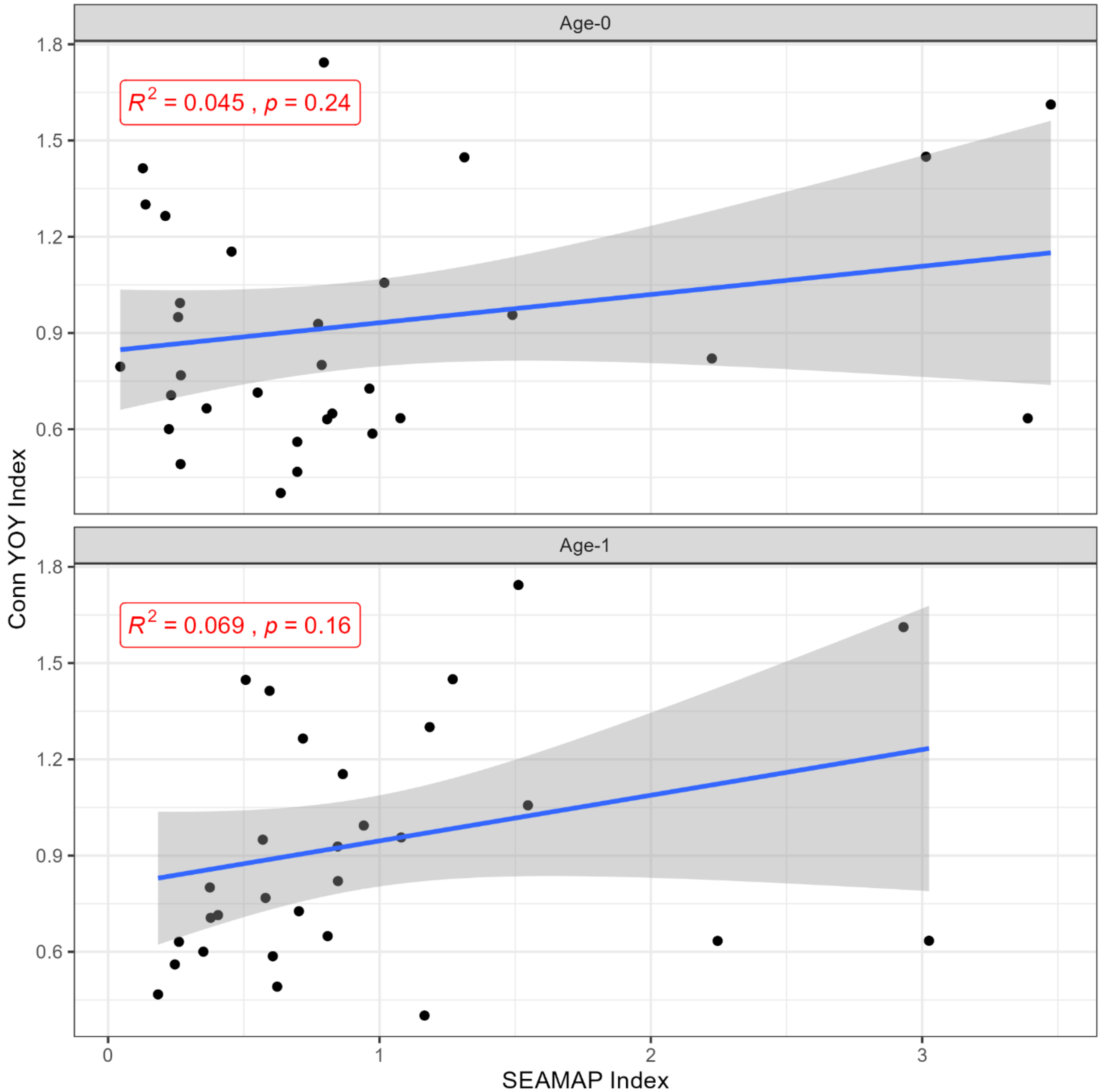

Figure 7. The composite YOY index plotted against the SEAMAP age-0 index (top) and the lagged SEAMAP age-1 index (bottom).

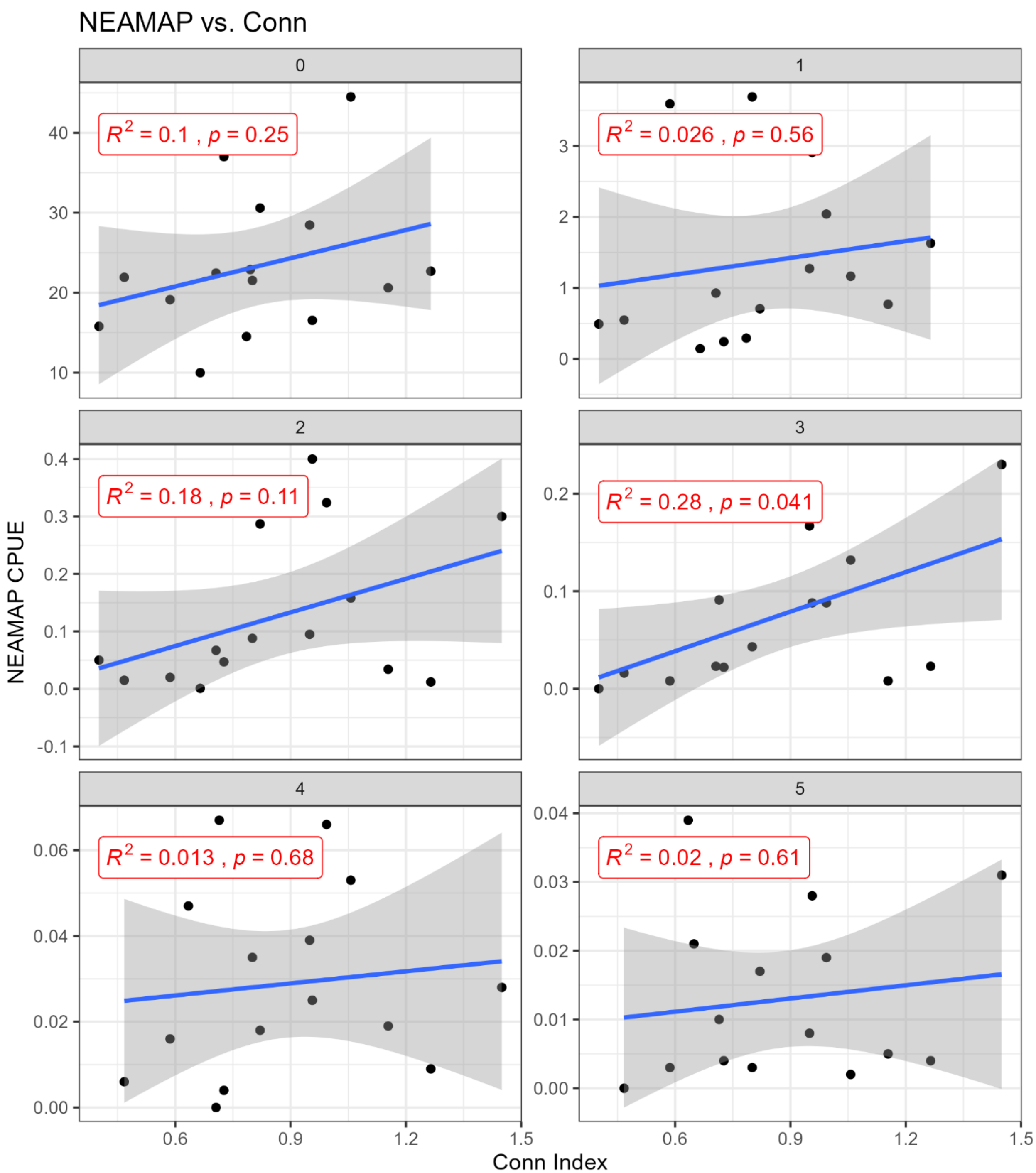

Figure 8. NEAMAP index-at-age plotted against the composite YOY index.

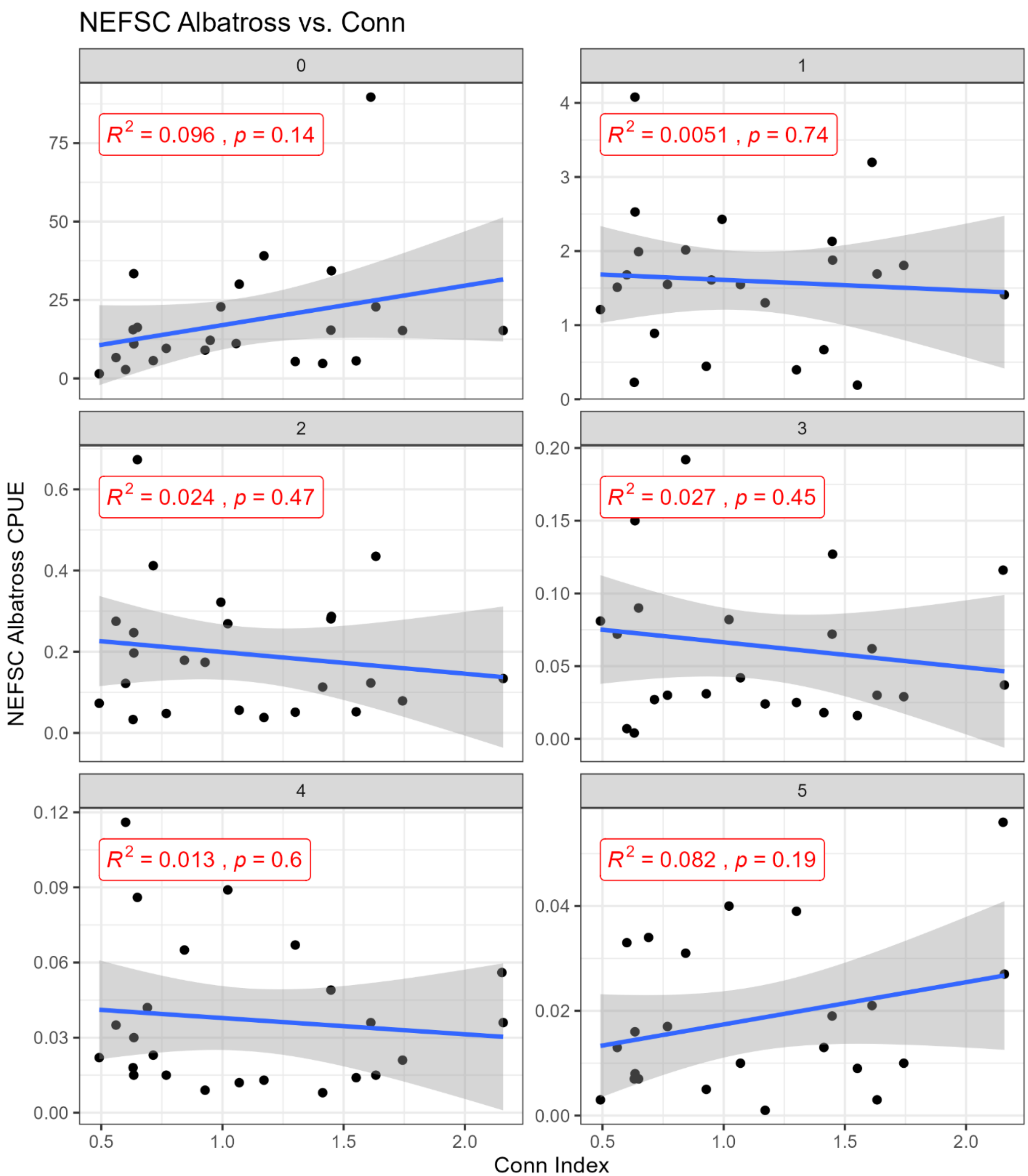

Figure 9. NEFSC Albatross index-at-age plotted against the composite YOY index.

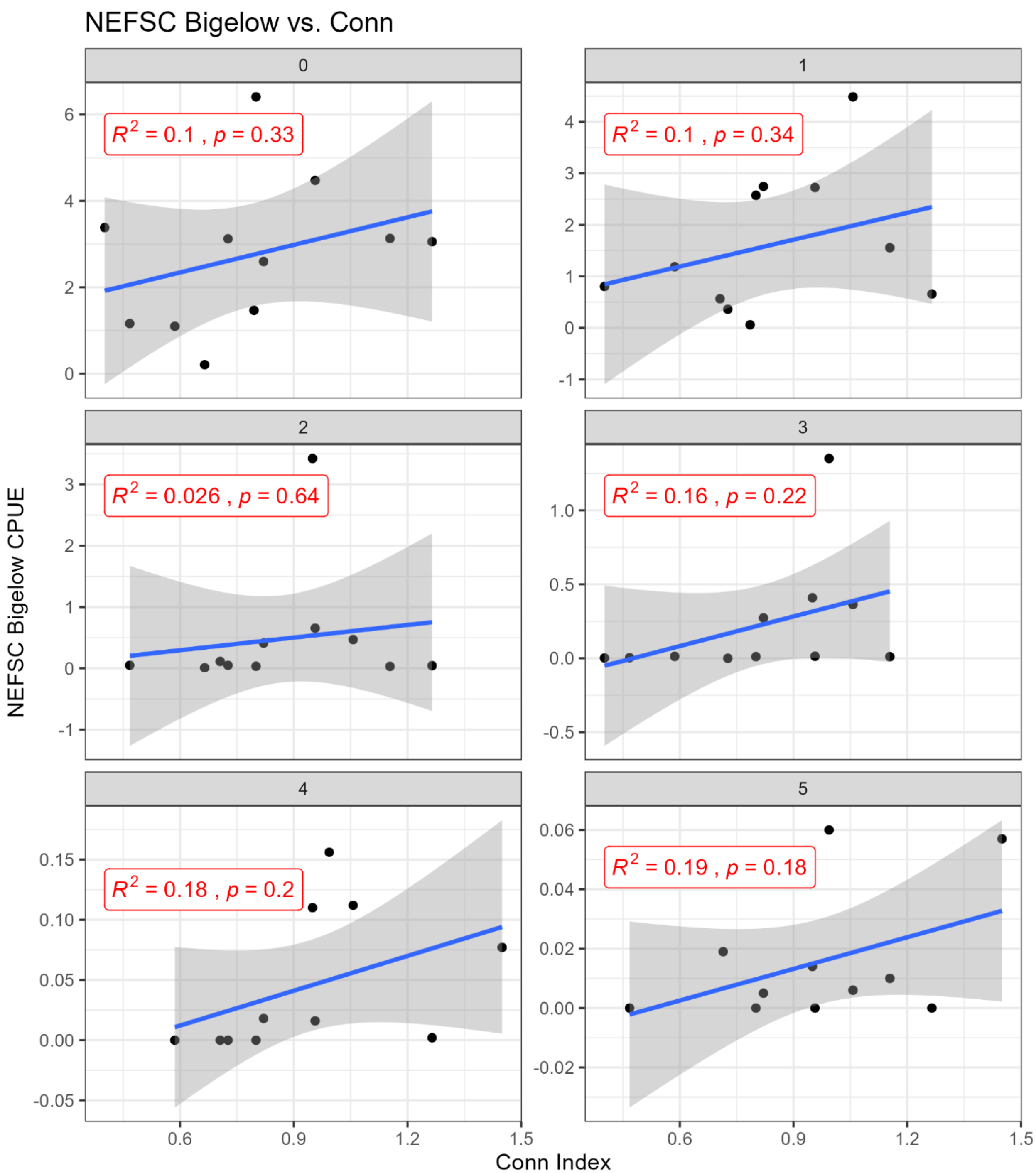

Figure 10. NEFSC Bigelow index-at-age plotted against the composite YOY index.

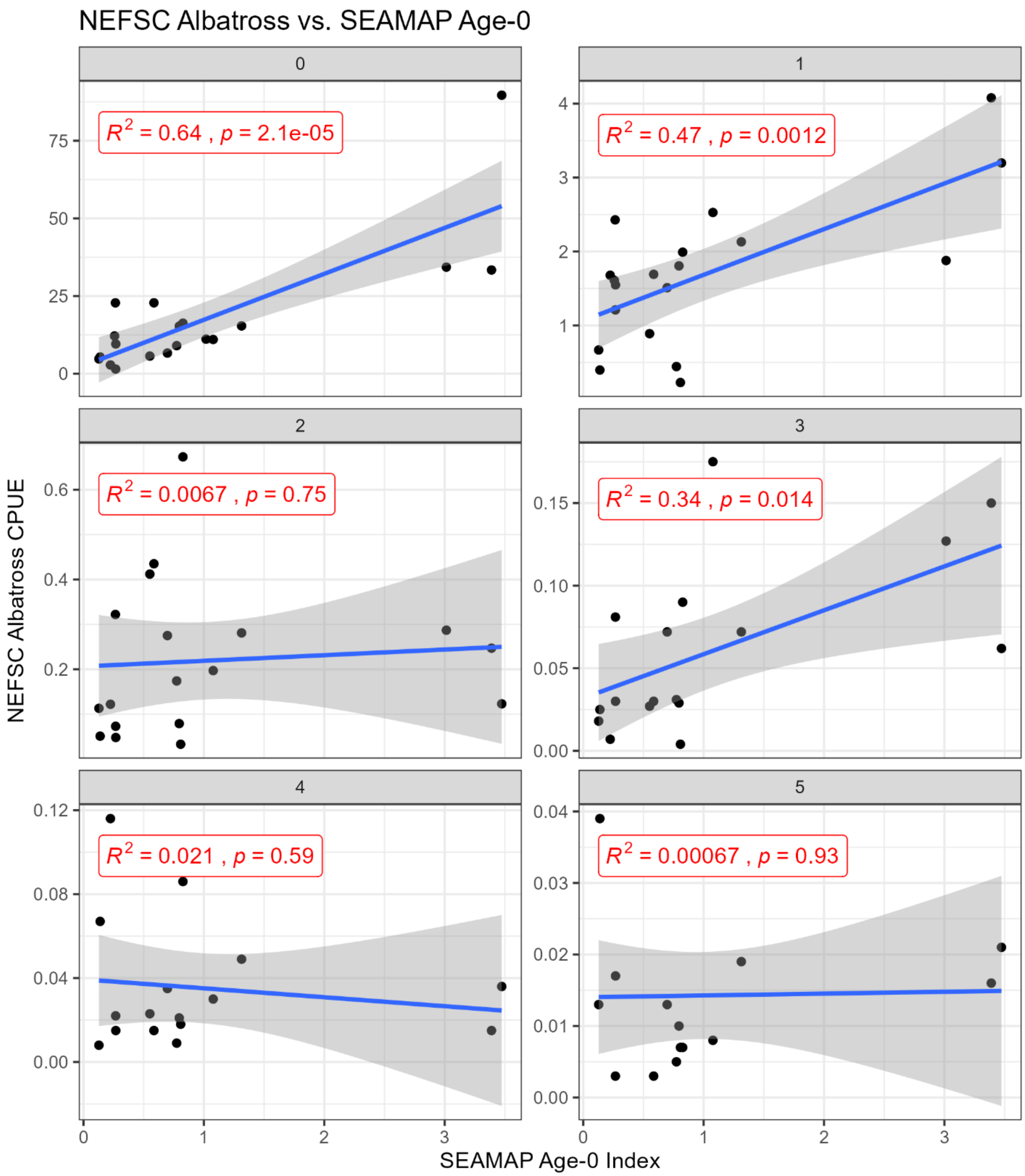

Figure 11. NEFSC Albatross index-at-age plotted against the SEAMAP age-0 index.

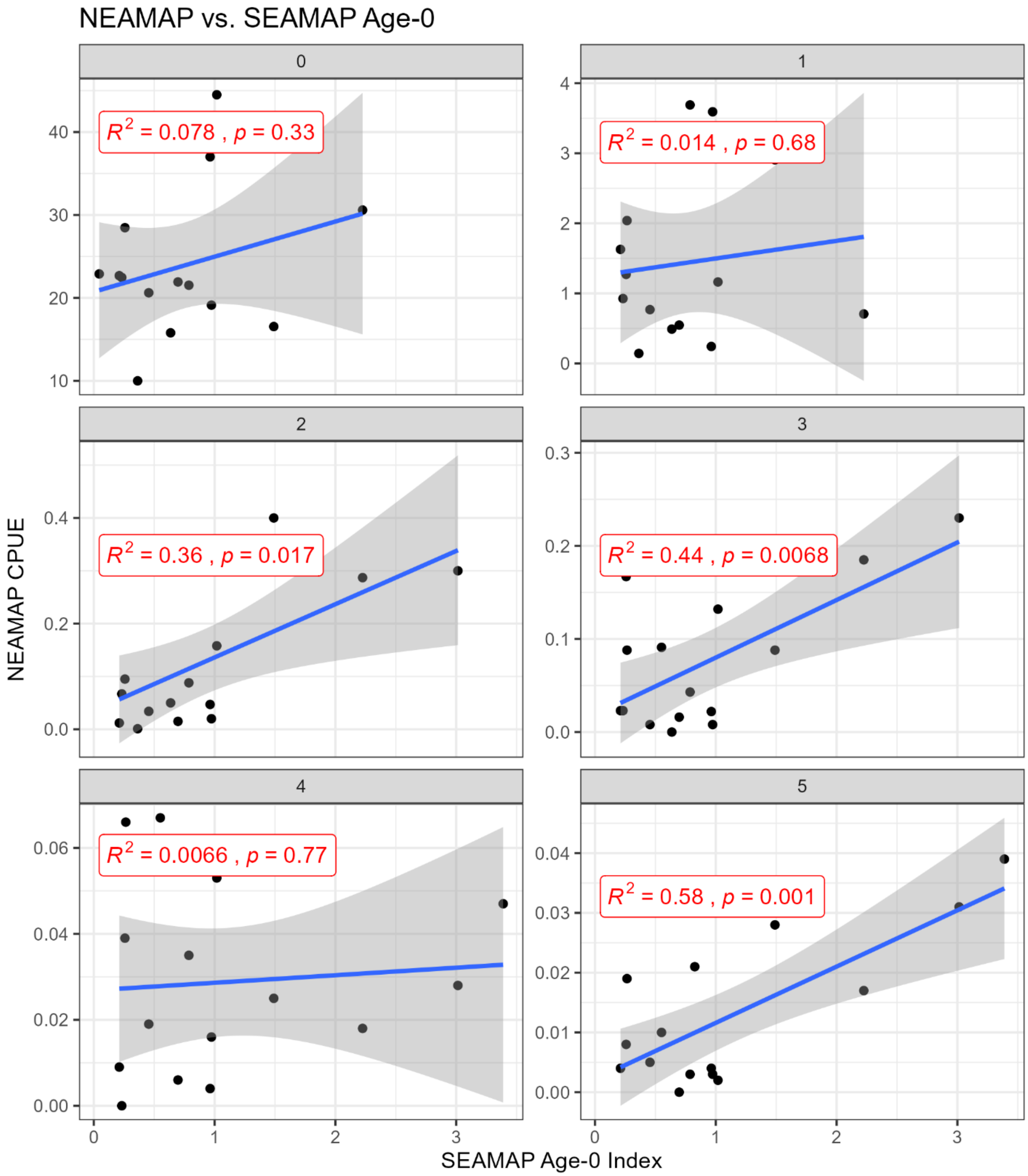

Figure 12. NEAMAP index-at-age plotted against the SEAMAP age-0 index.

Appendix 1: Diagnostic Plots

The underlying equation for the Conn model is:

$$\log(U_t) \sim Normal(\log(\mu_t) + \chi_i, \left(\sigma_i^p\right)^2 + \left(\sigma_{it}^S\right)^2)$$

Where
μ_t = the underlying population abundance in year *t*
χ_i = the catchability of survey *i*
σ_i^p = the process error for survey *i*
σ_{it}^S = the sampling error for survey *i* in year *t*

σ_{it}^S is input from the annual survey CVs, while all other parameters are estimated.

Trace plots, autocorrelation plots, running means, and density plots are provided for each parameter estimate.

The χ_i plots are labeled as chi[1] – chi[6], indexing the surveys from north to south (NH – VA).
The μ_t plots are labeled mu[1] – mu[41], indexing years 1981-2021.
The σ_i^p plots are labeled sigma[1] – sigma[6], indexing the surveys from north to south (NH – VA).

Diagnostics for chi[1]

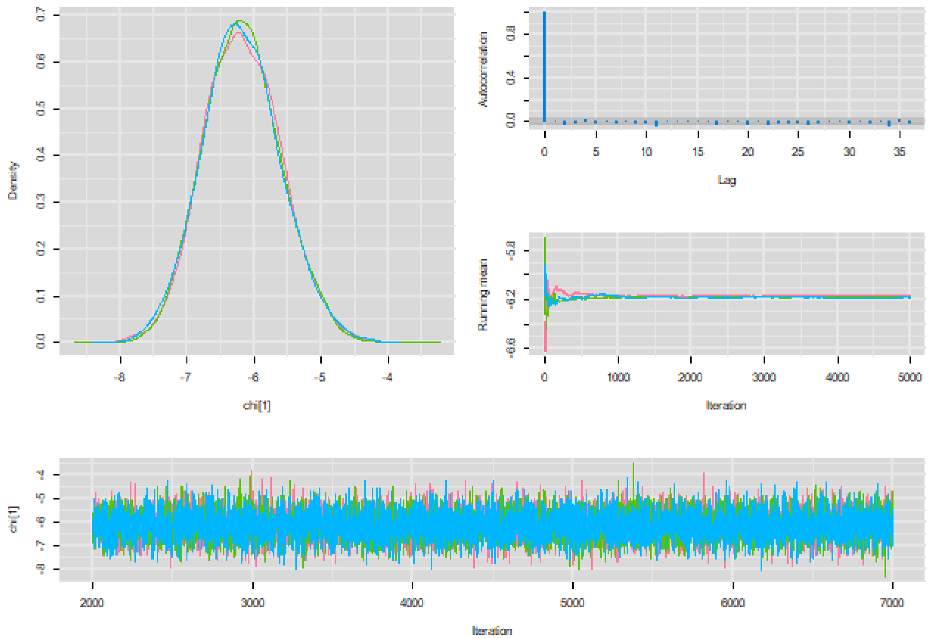

Diagnostics for chi[2]

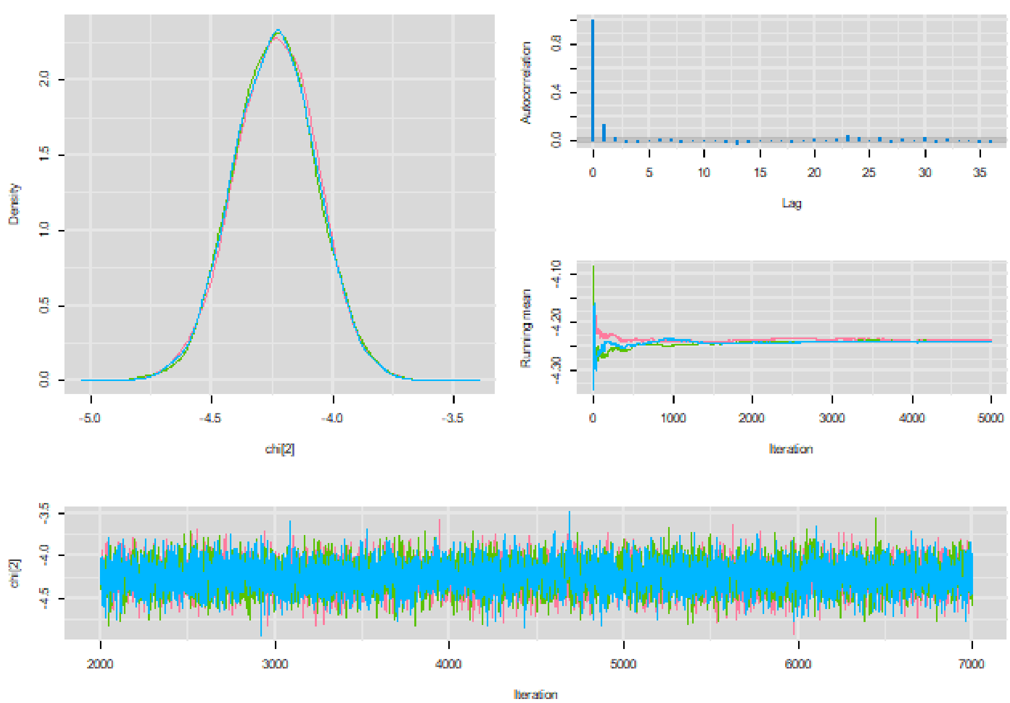

Diagnostics for chi[3]

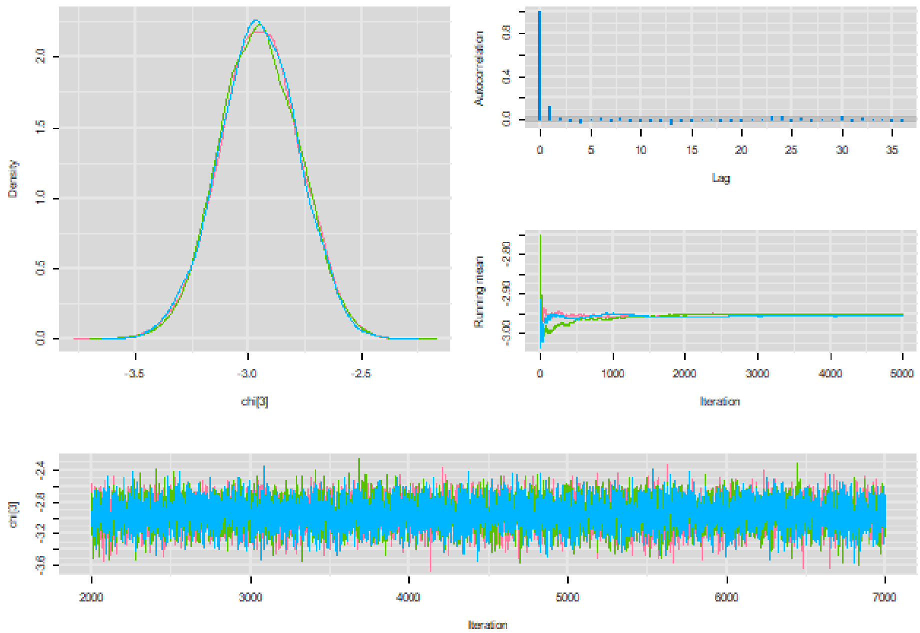

Diagnostics for chi[4]

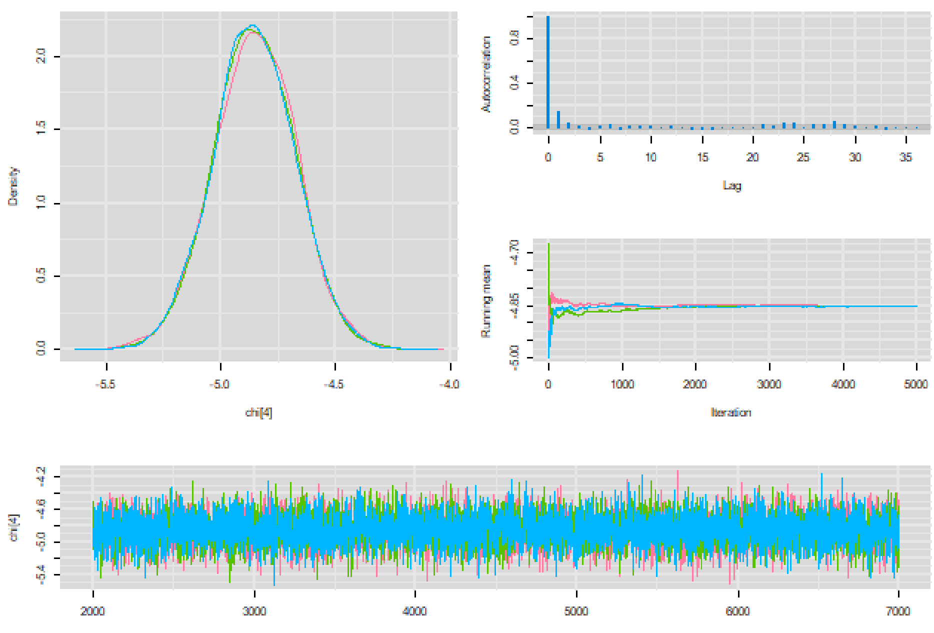

Diagnostics for chi[5]

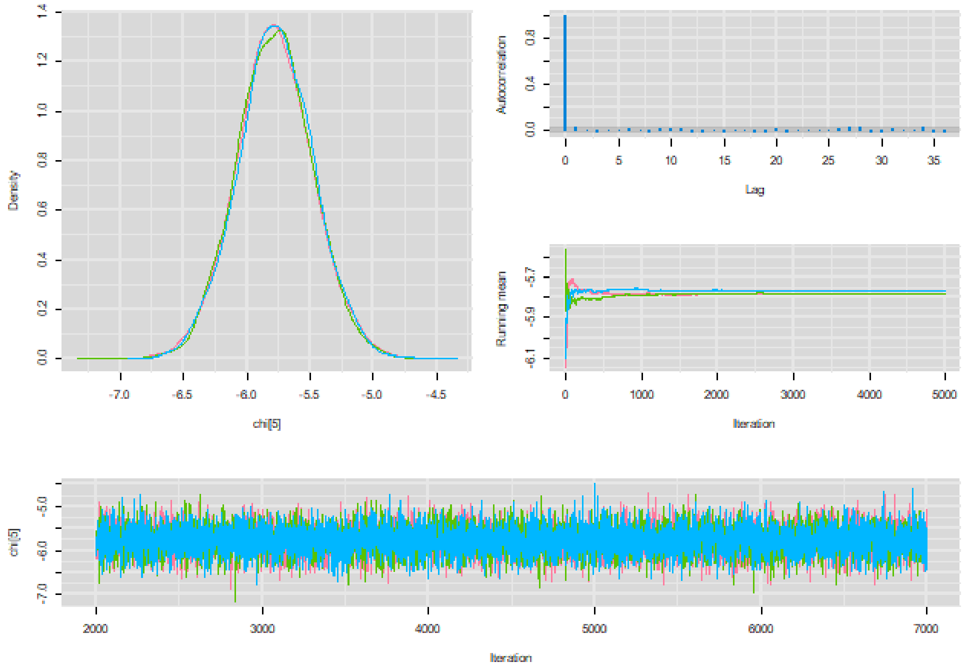

Diagnostics for chi[6]

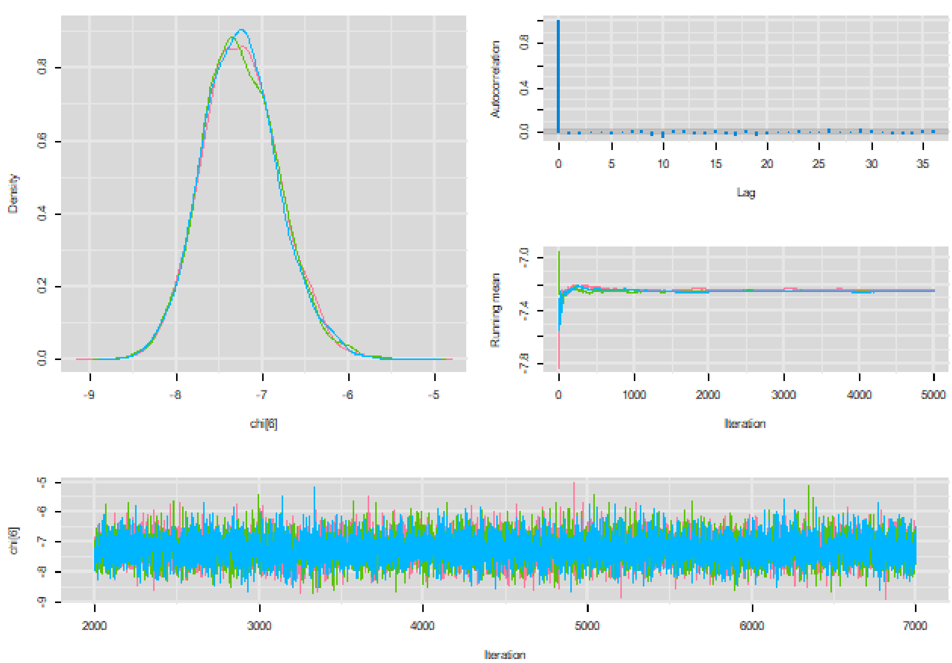

Diagnostics for deviance

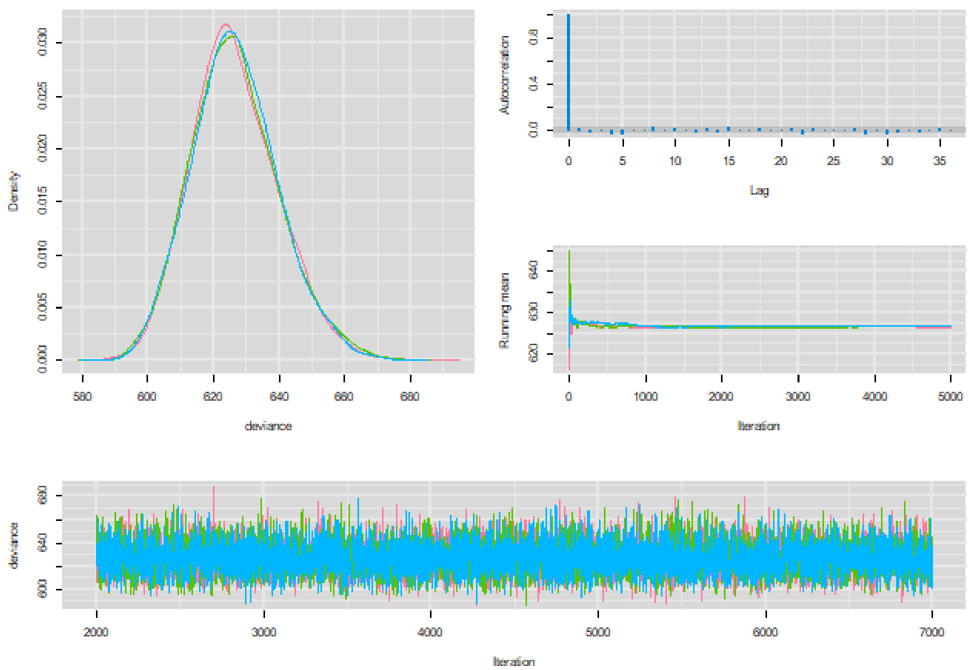

Diagnostics for mu[1]

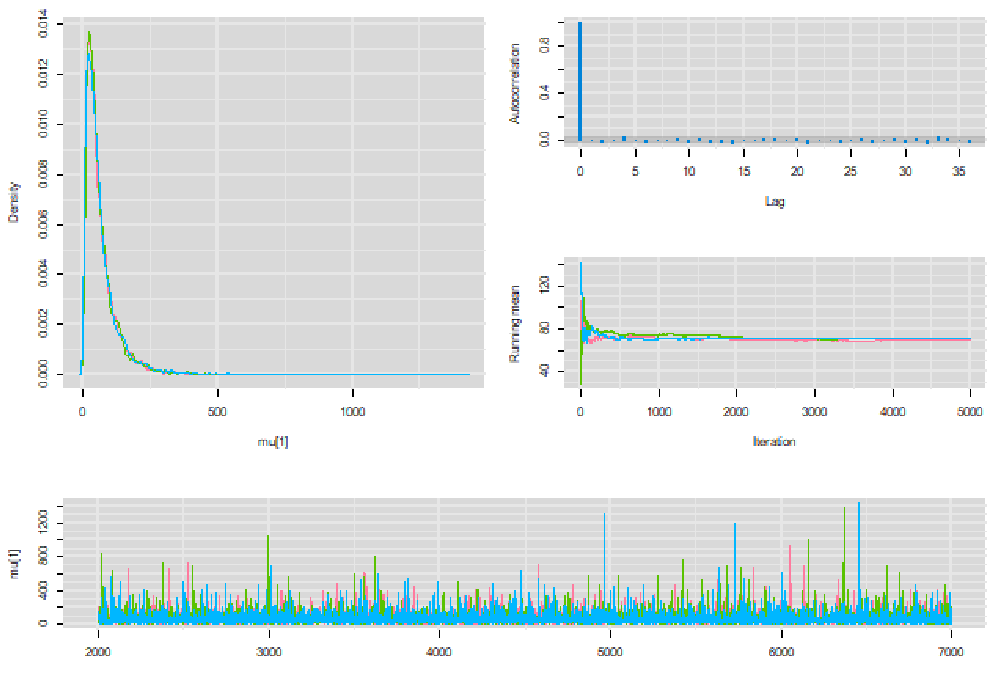

Diagnostics for mu[2]

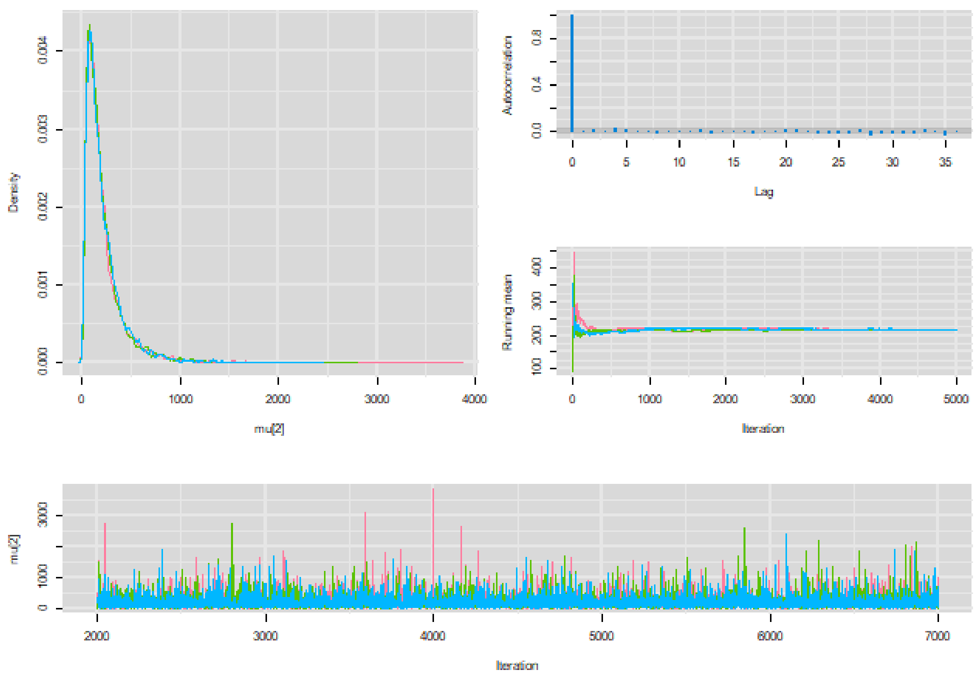

Diagnostics for mu[3]

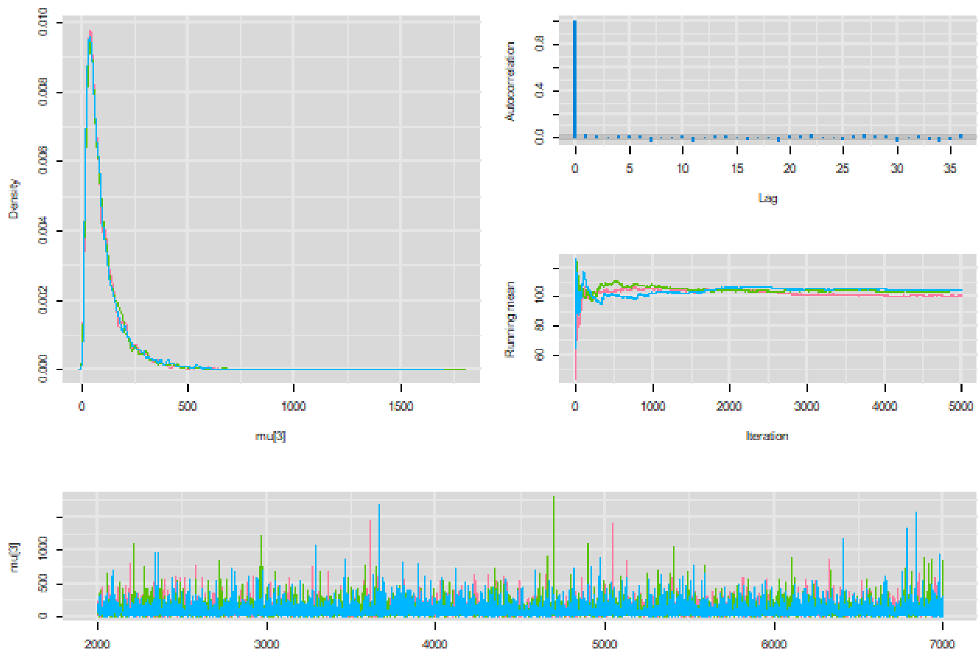

Diagnostics for mu[4]

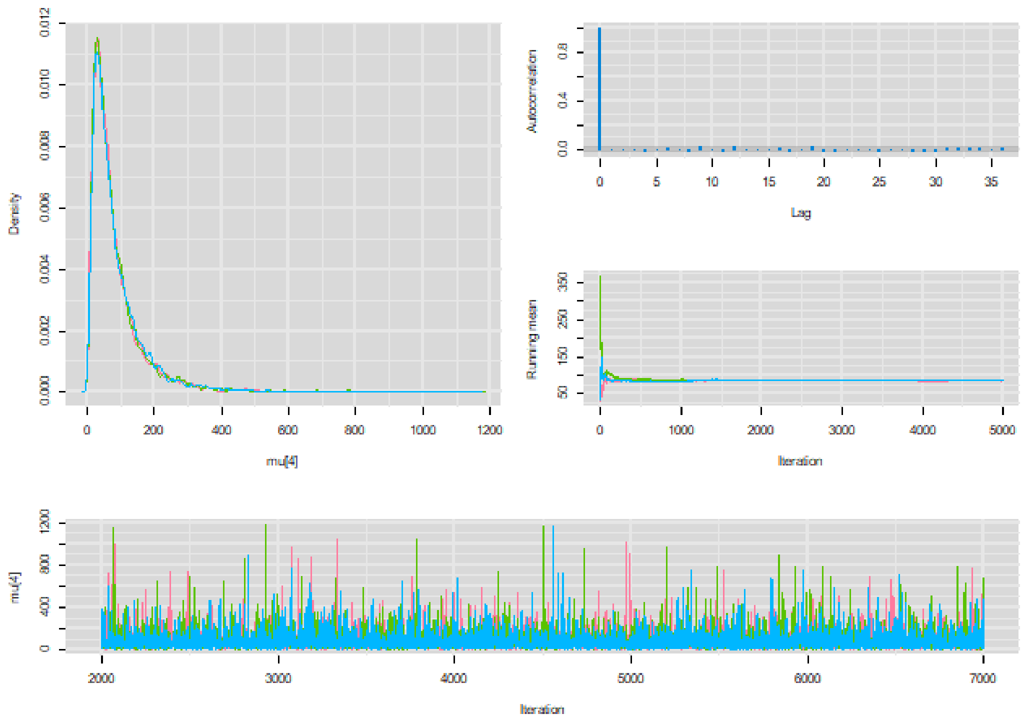

Diagnostics for mu[5]

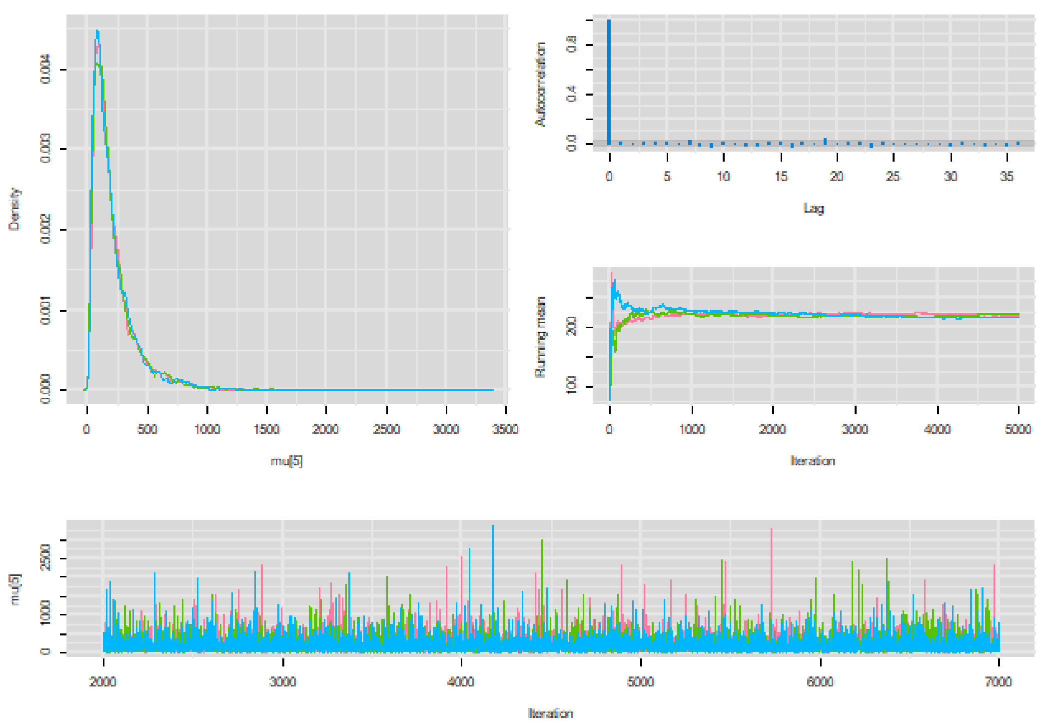

Diagnostics for mu[6]

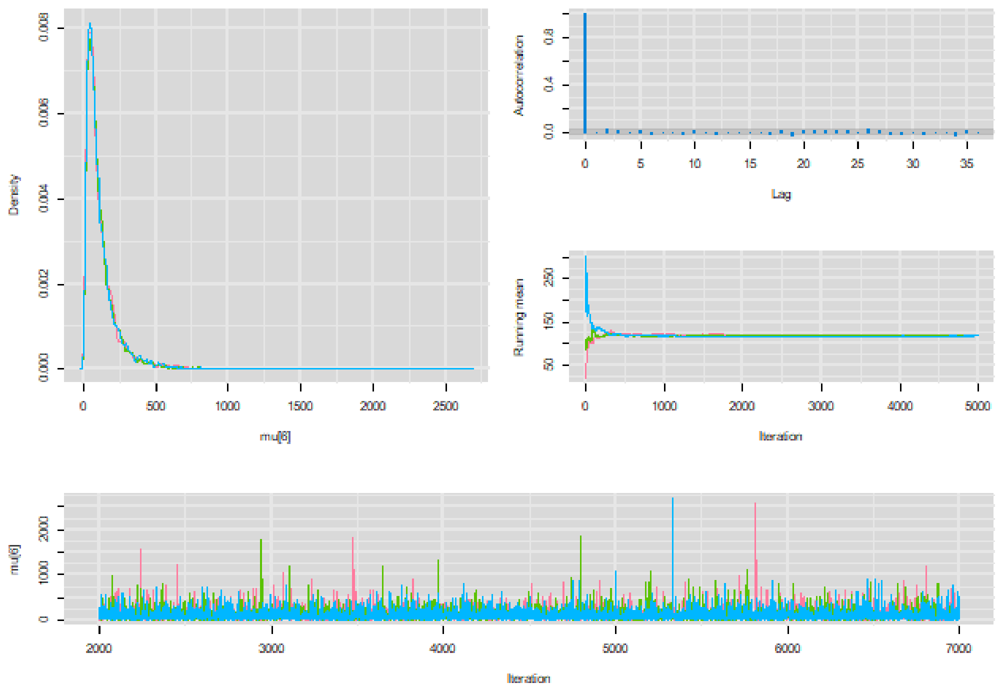

Diagnostics for mu[7]

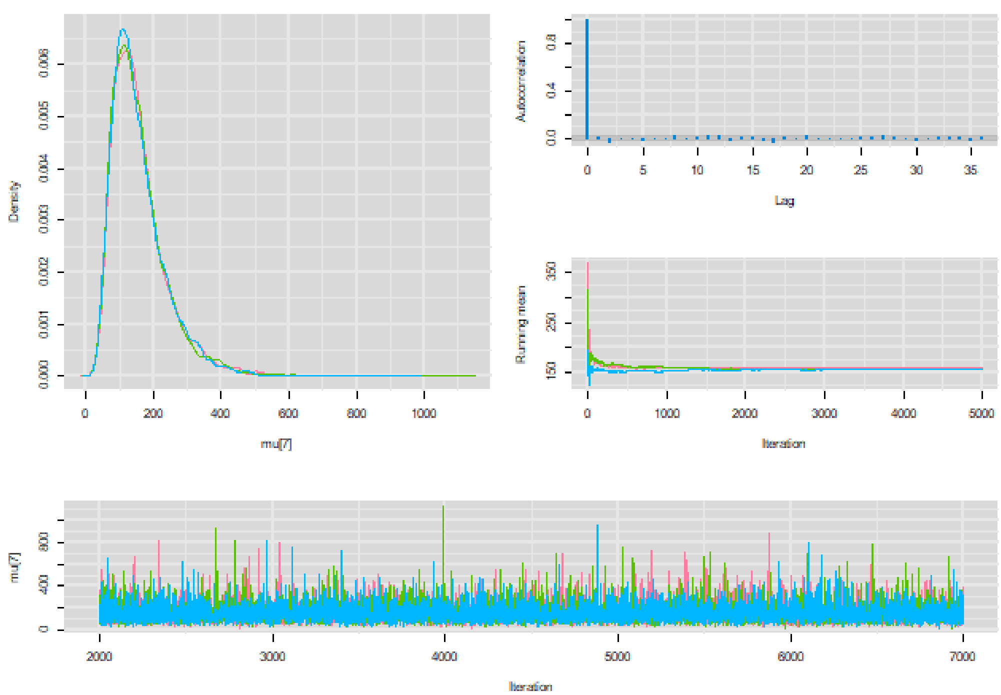

Diagnostics for mu[8]

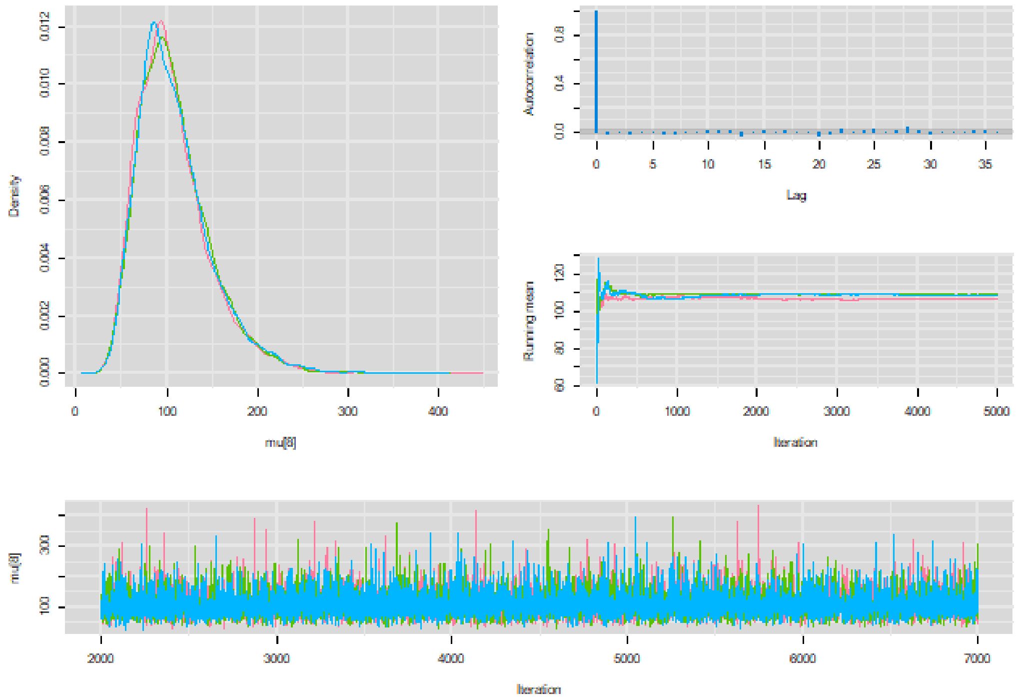

Diagnostics for mu[9]

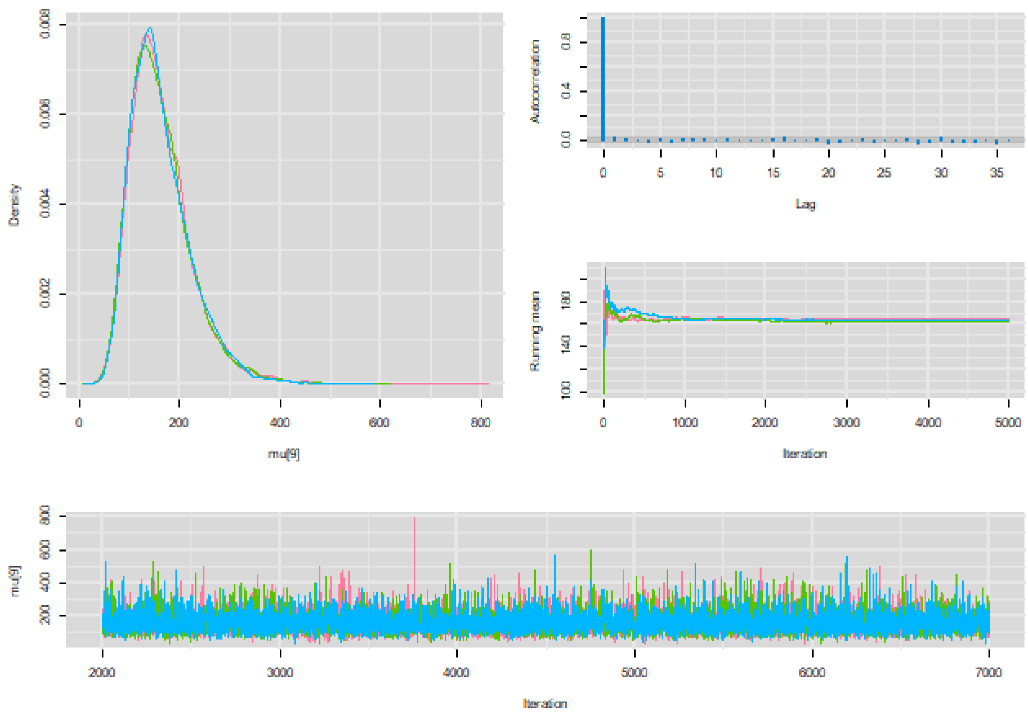

Diagnostics for mu[10]

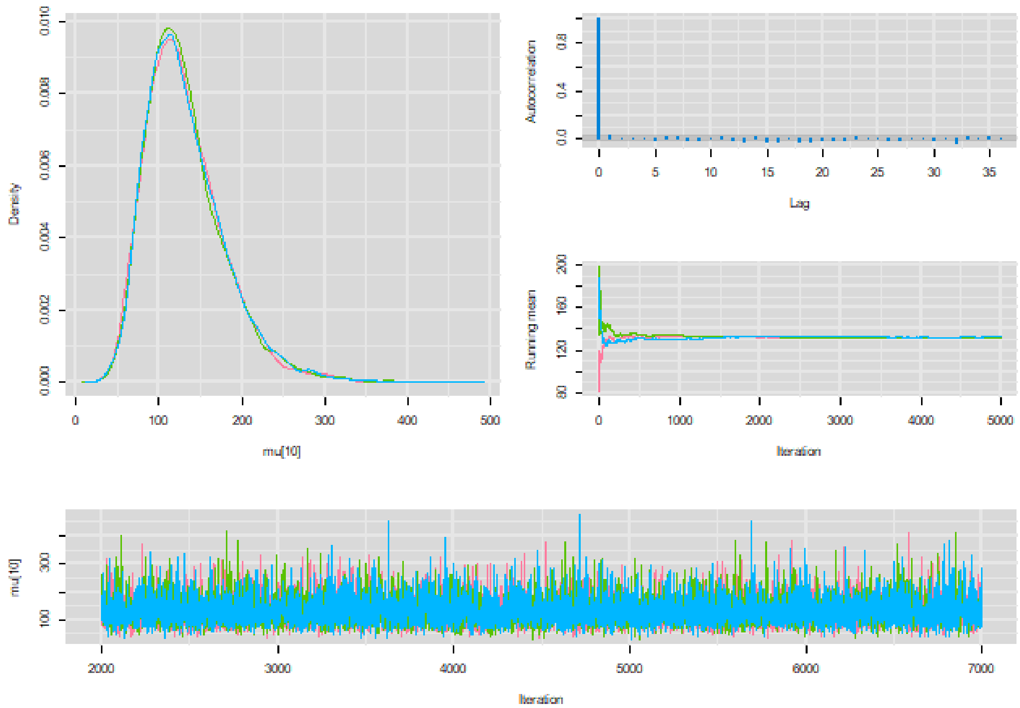

Diagnostics for mu[11]

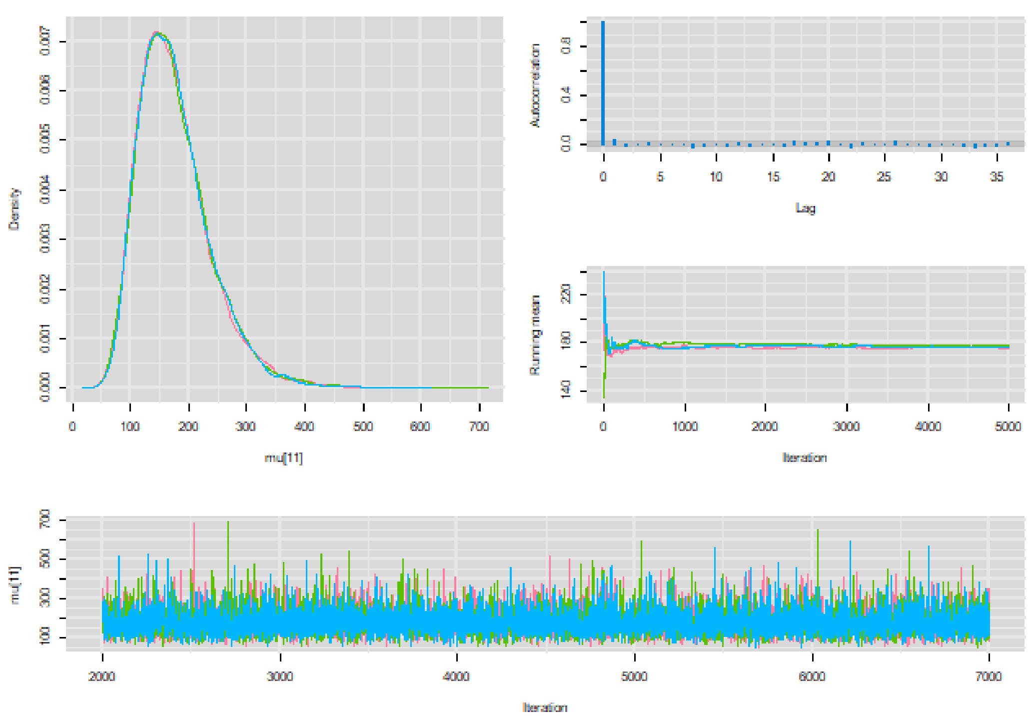

Diagnostics for mu[12]

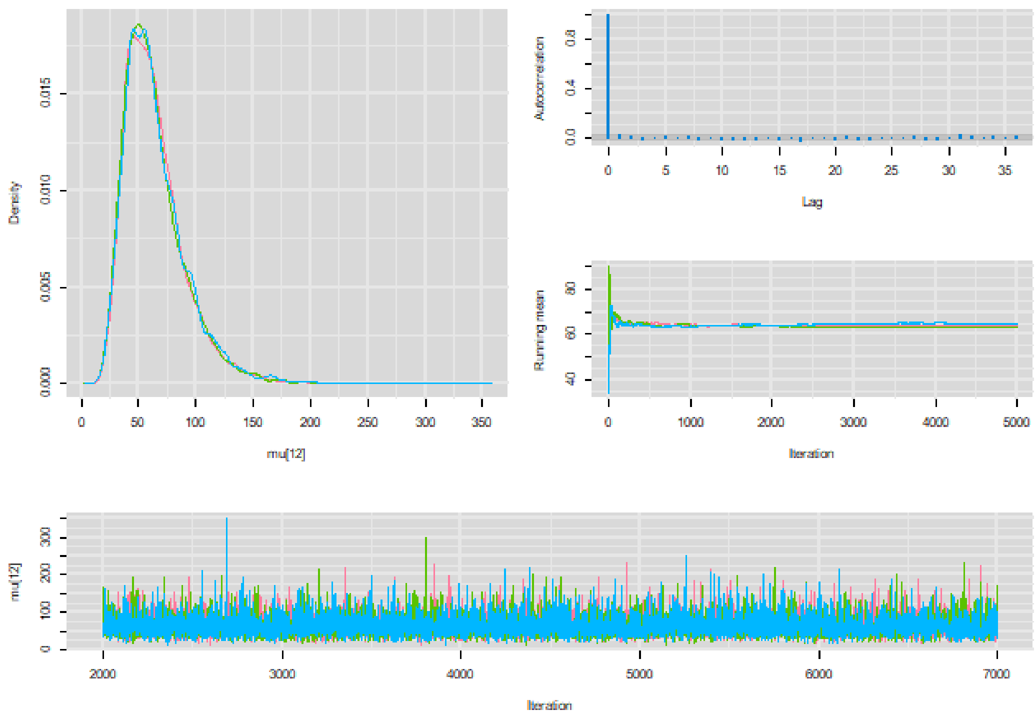

Diagnostics for mu[13]

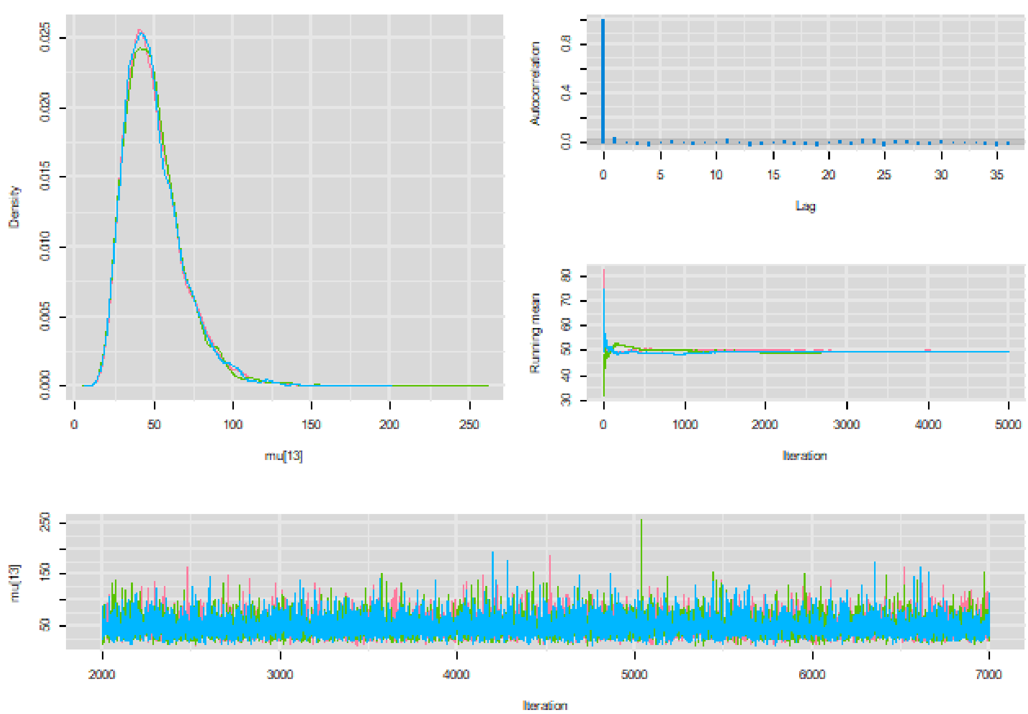

Diagnostics for mu[14]

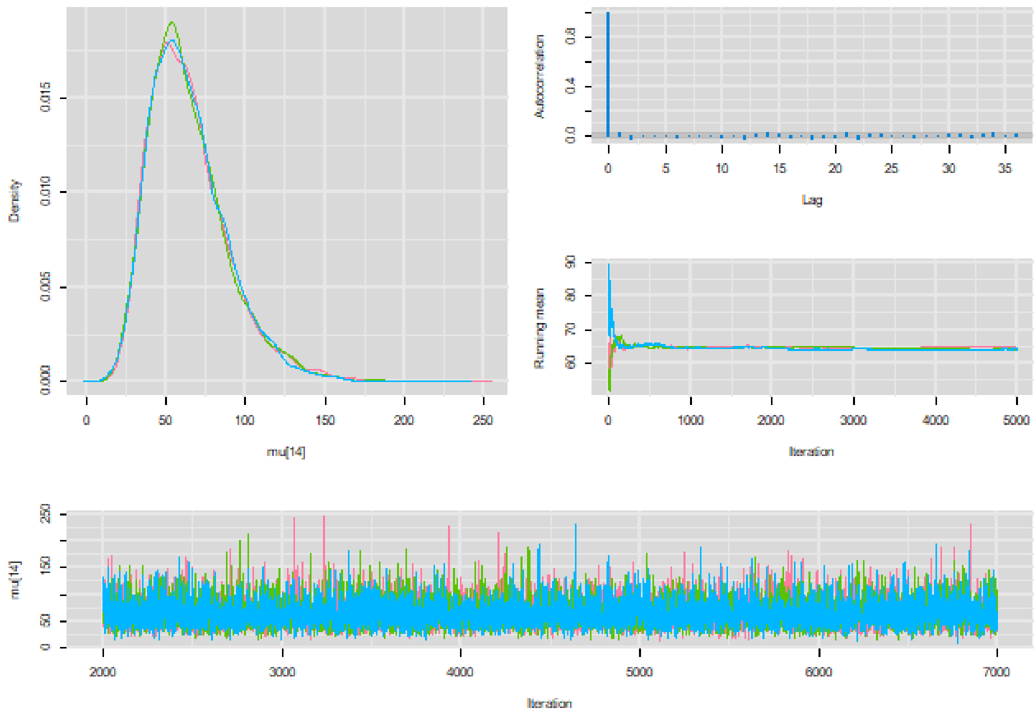

Diagnostics for mu[15]

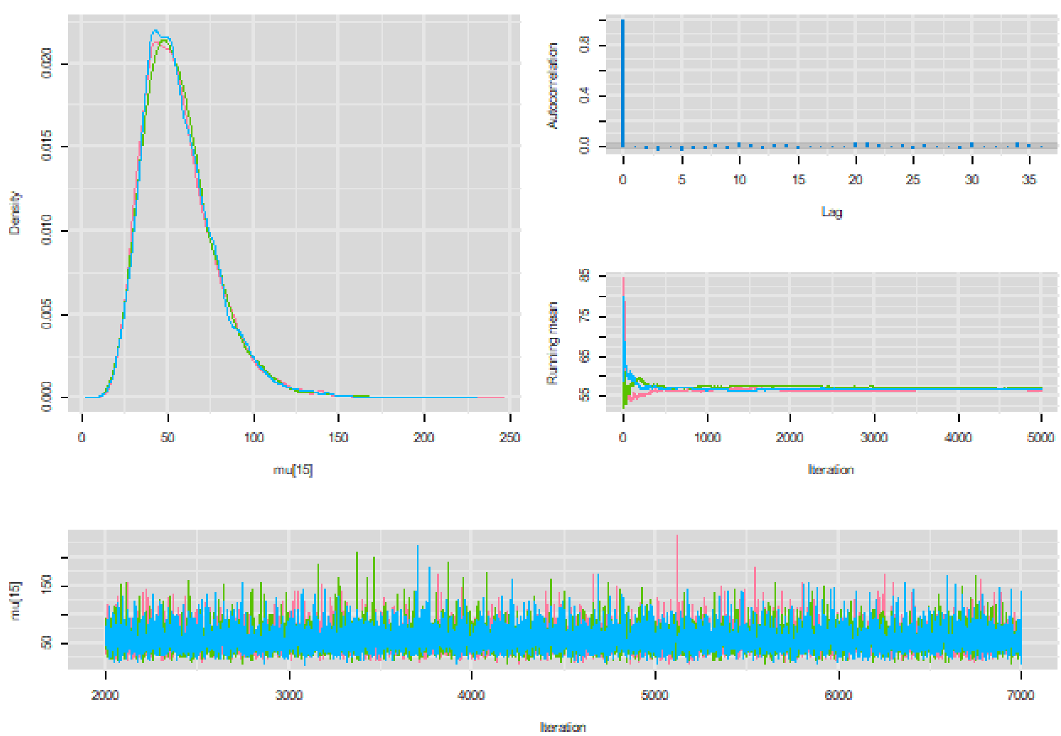

Diagnostics for mu[16]

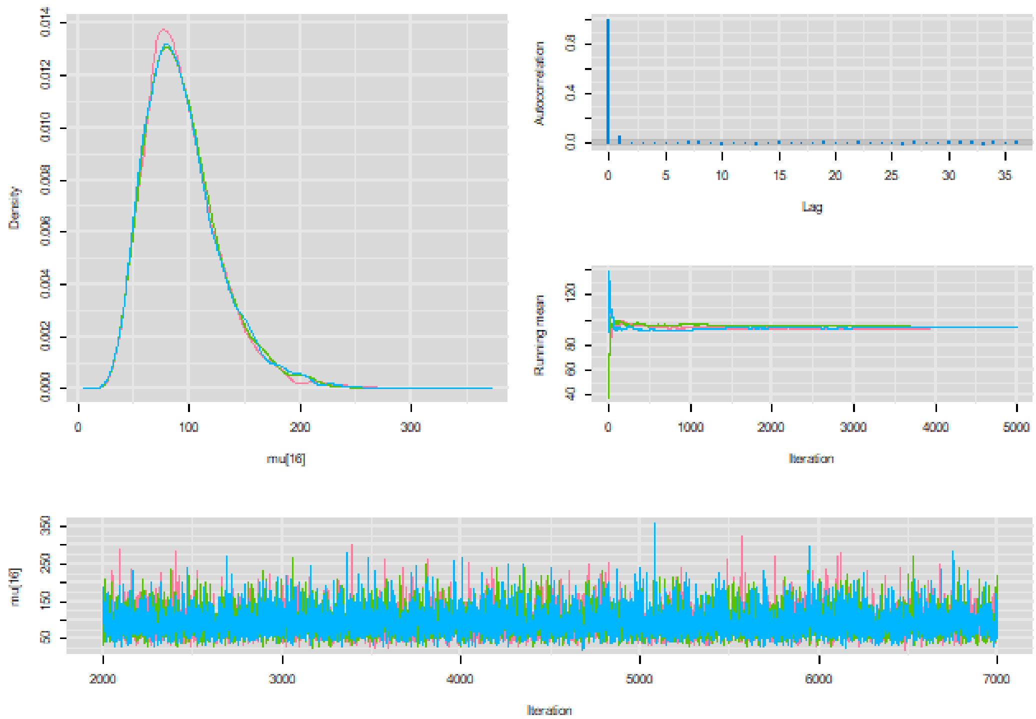

Diagnostics for mu[17]

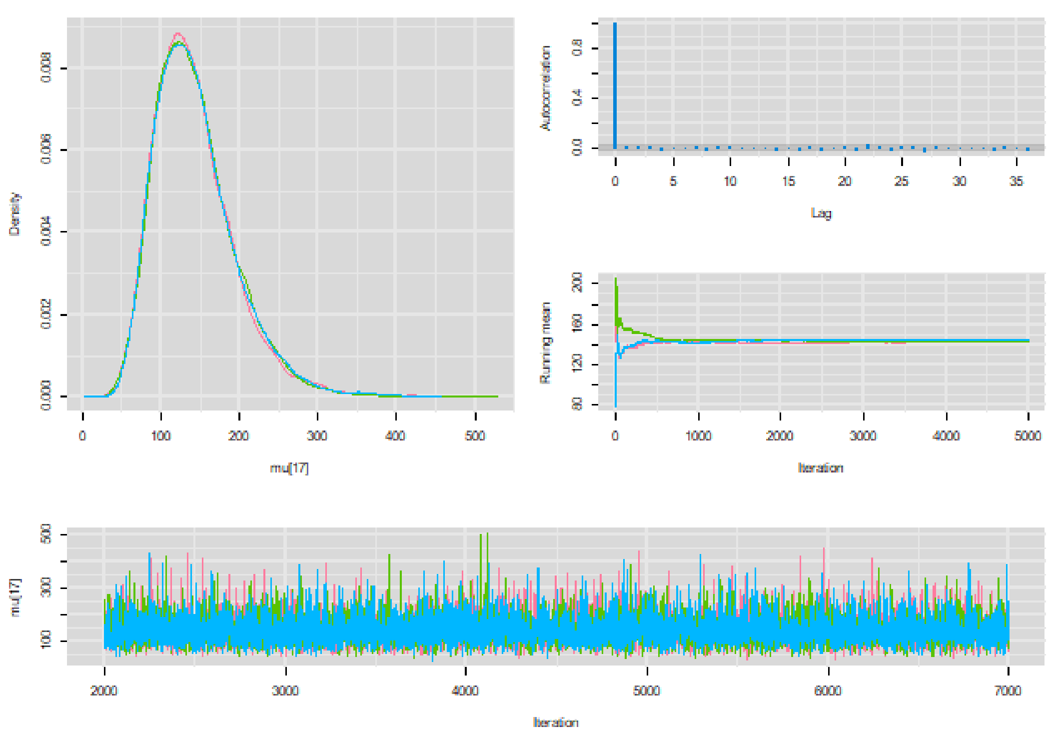

Diagnostics for mu[18]

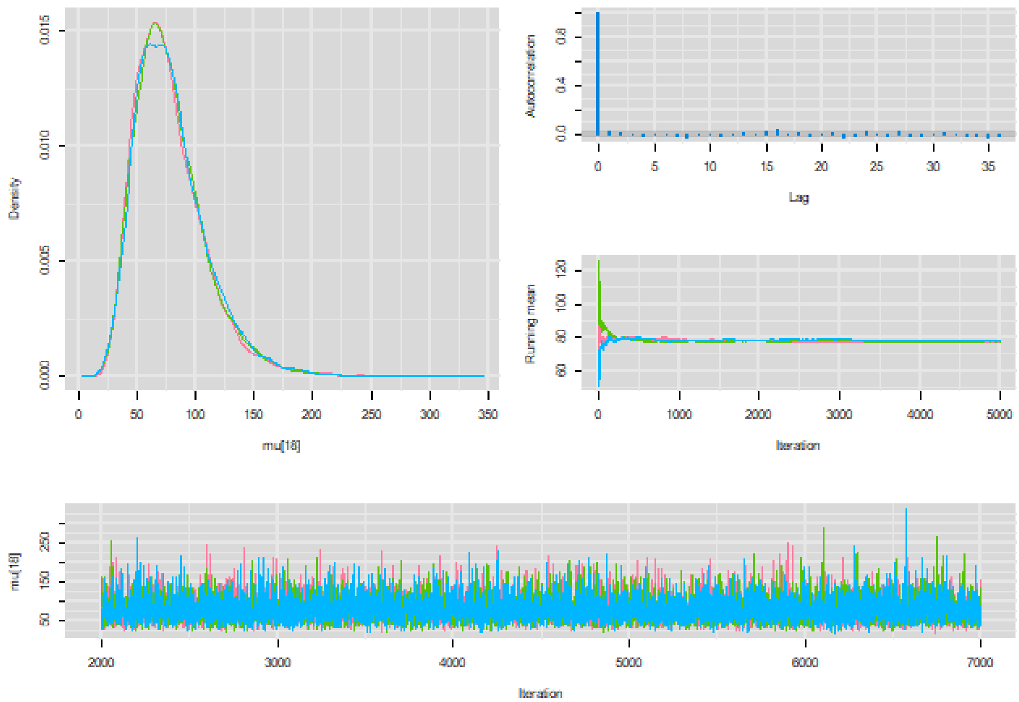

Diagnostics for mu[19]

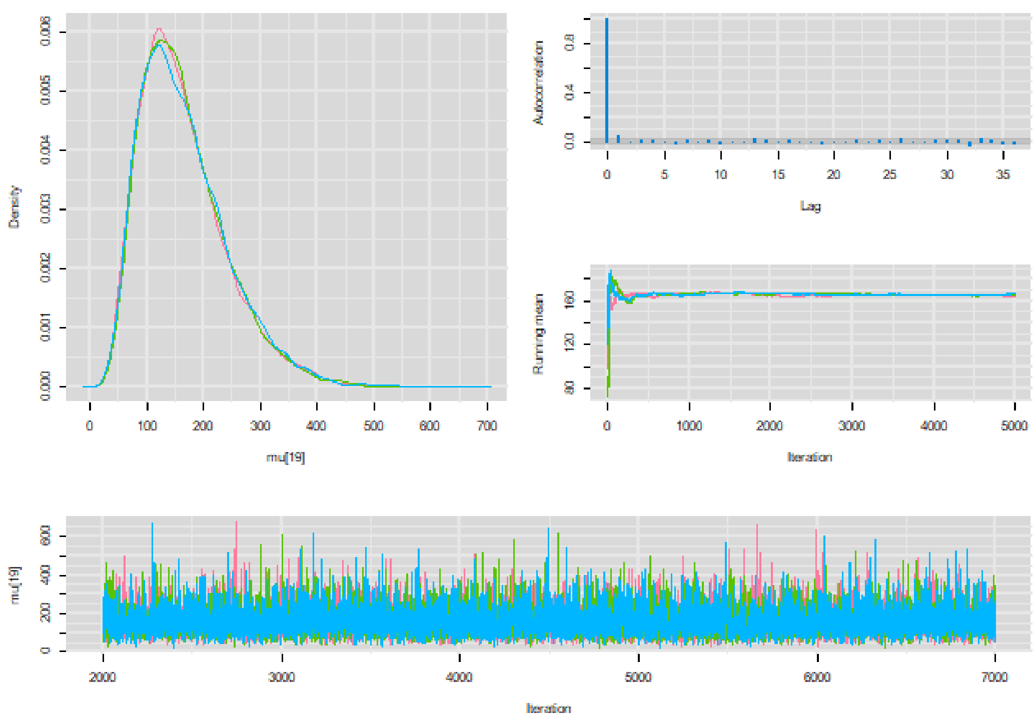

Diagnostics for mu[20]

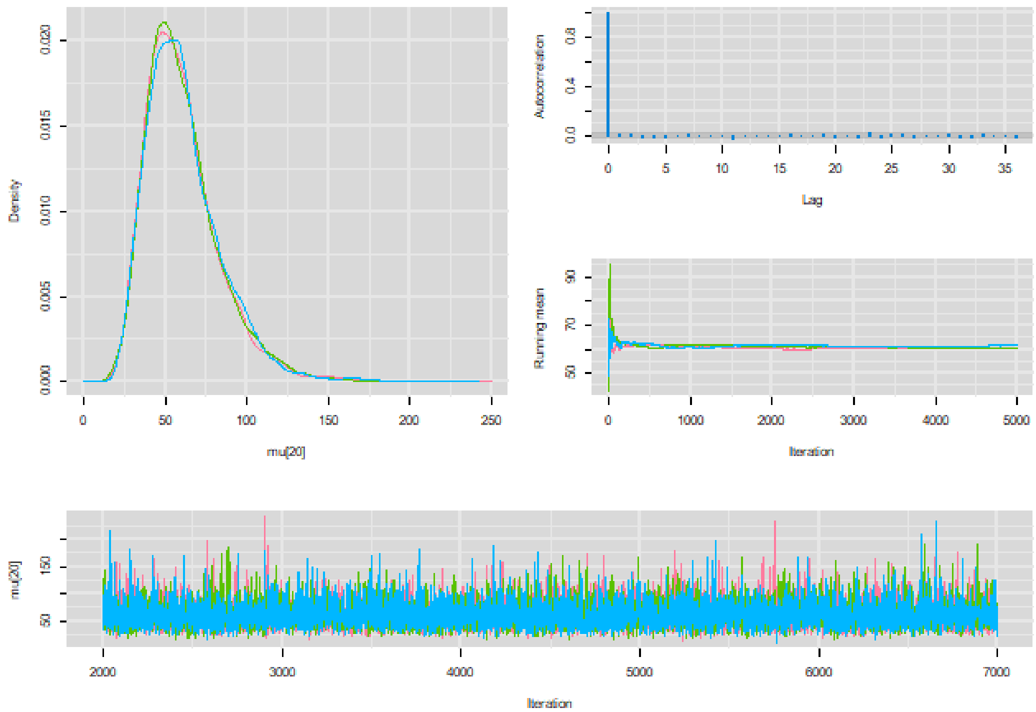

Diagnostics for mu[21]

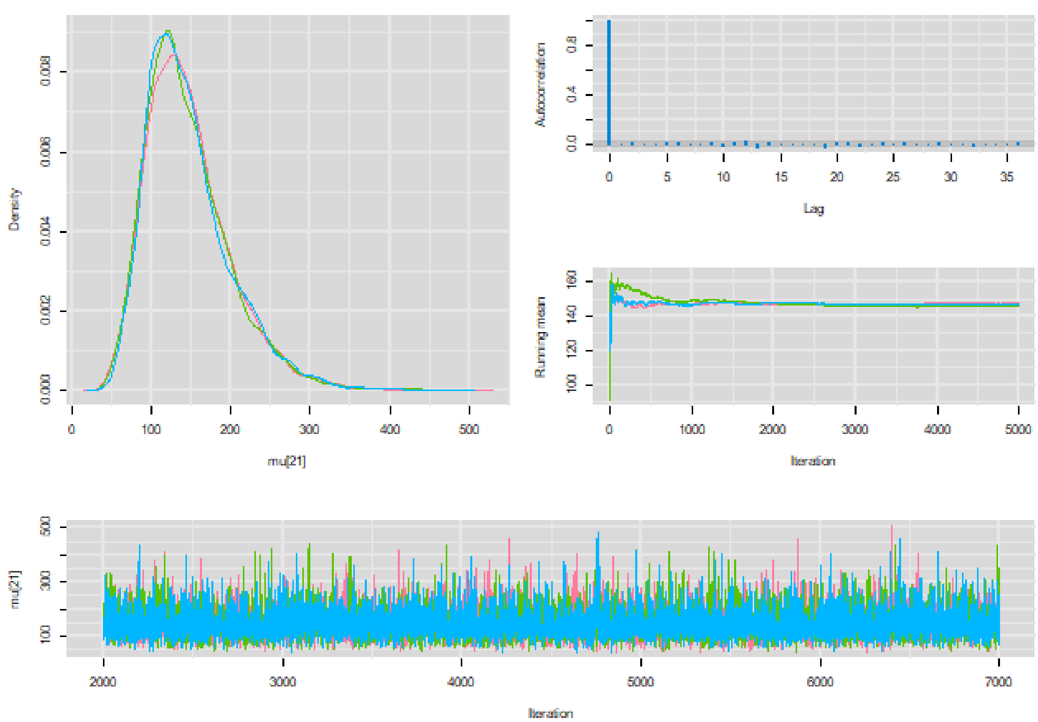

Diagnostics for mu[22]

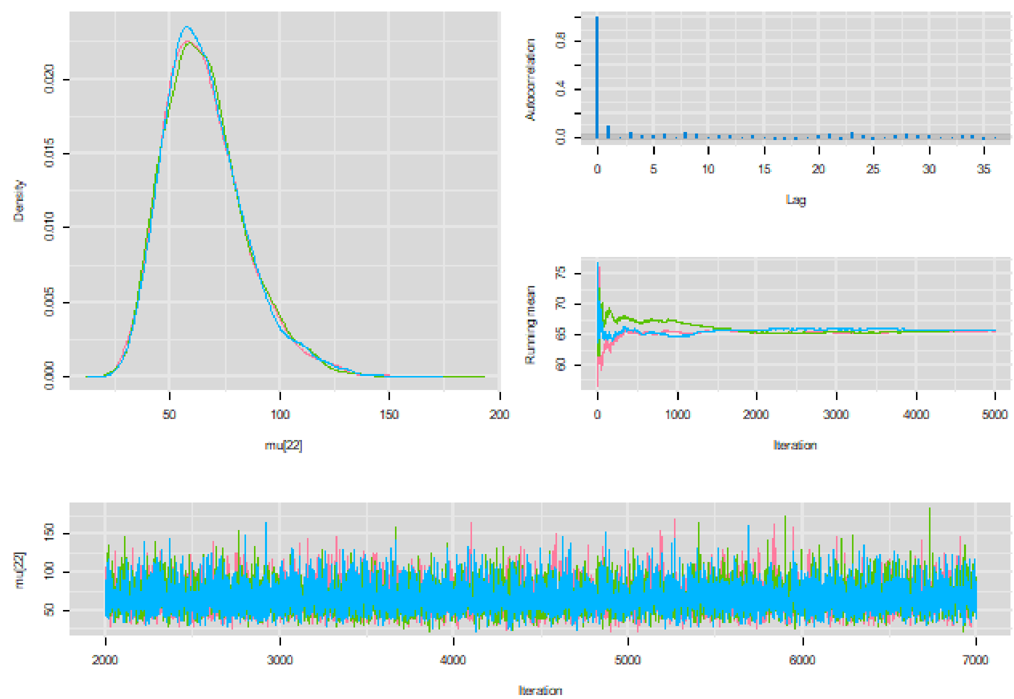

Diagnostics for mu[23]

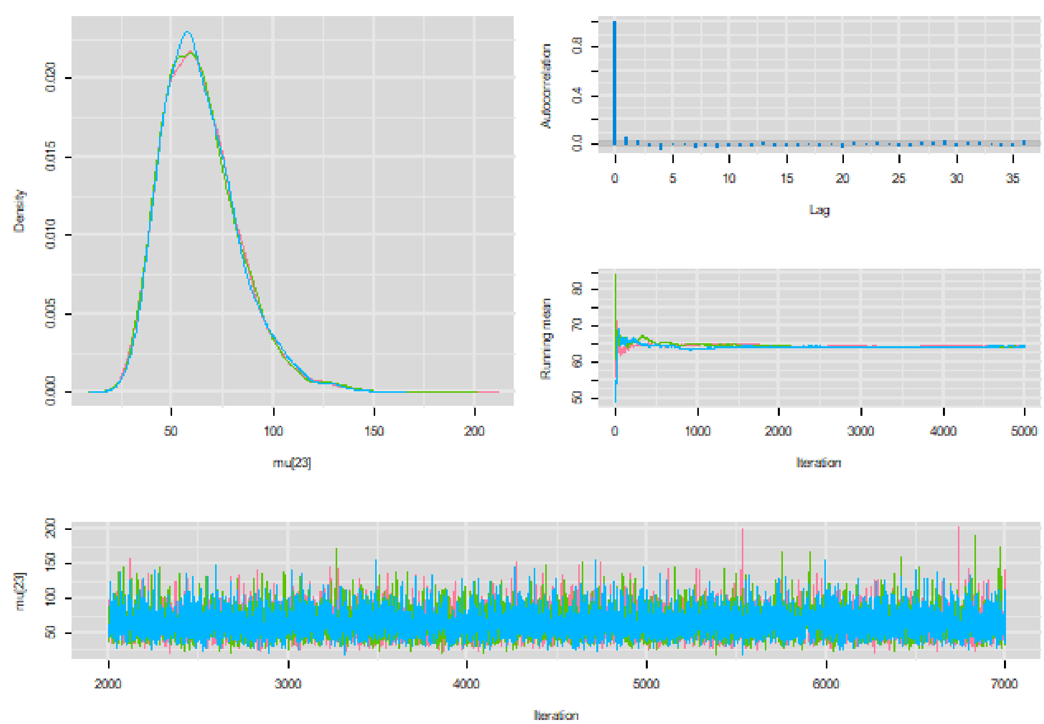

Diagnostics for mu[24]

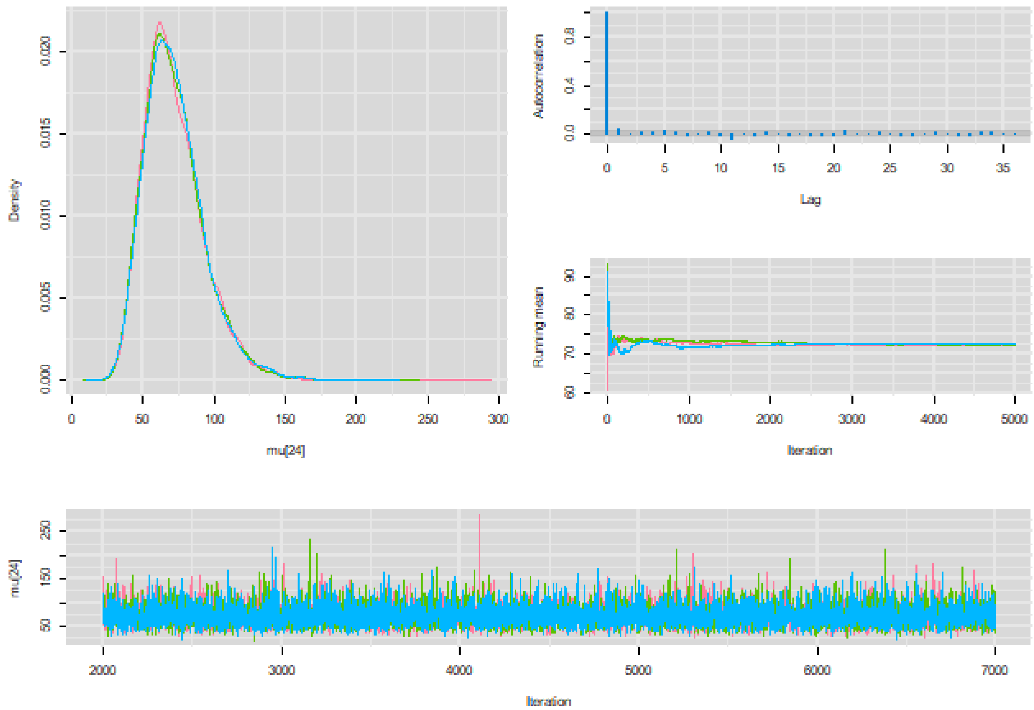

Diagnostics for mu[25]

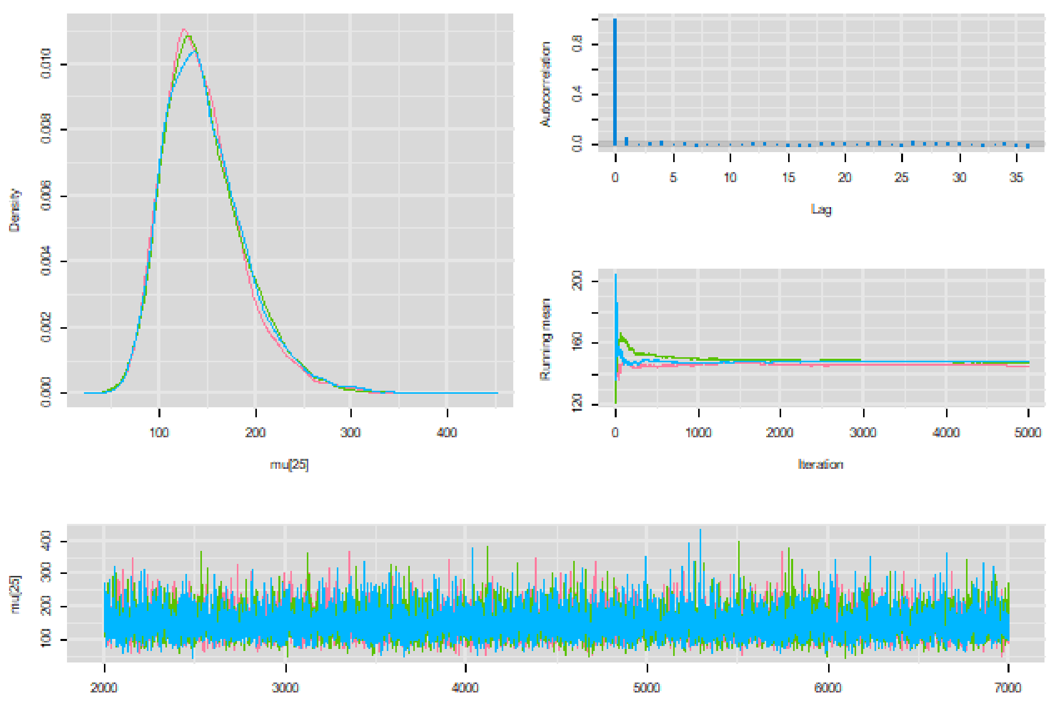

Diagnostics for mu[26]

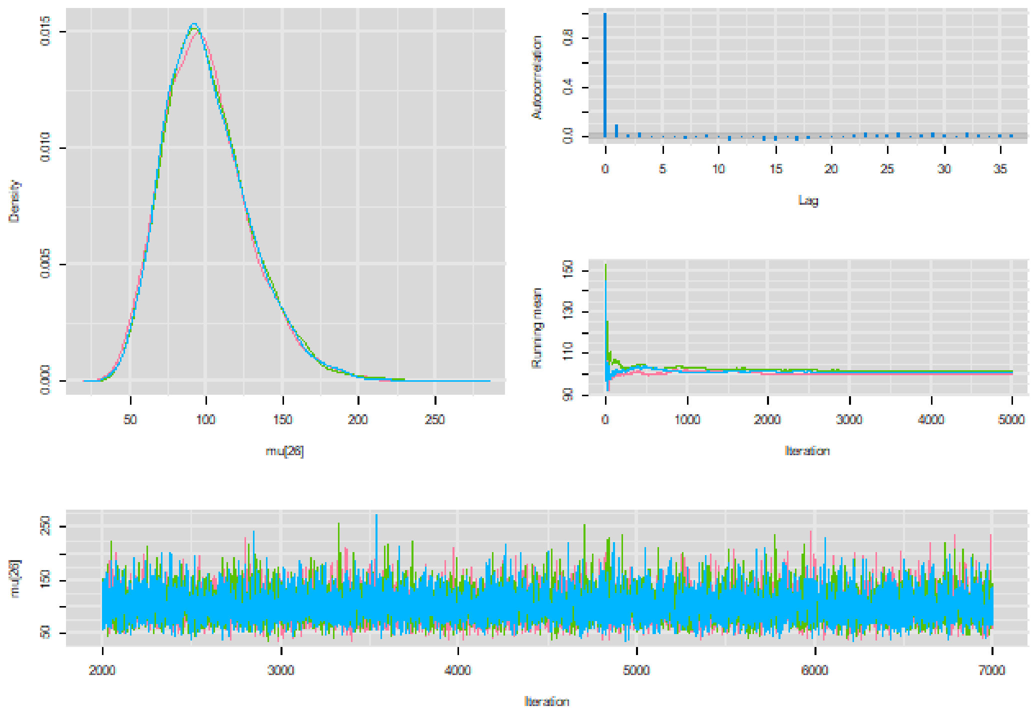

Diagnostics for mu[27]

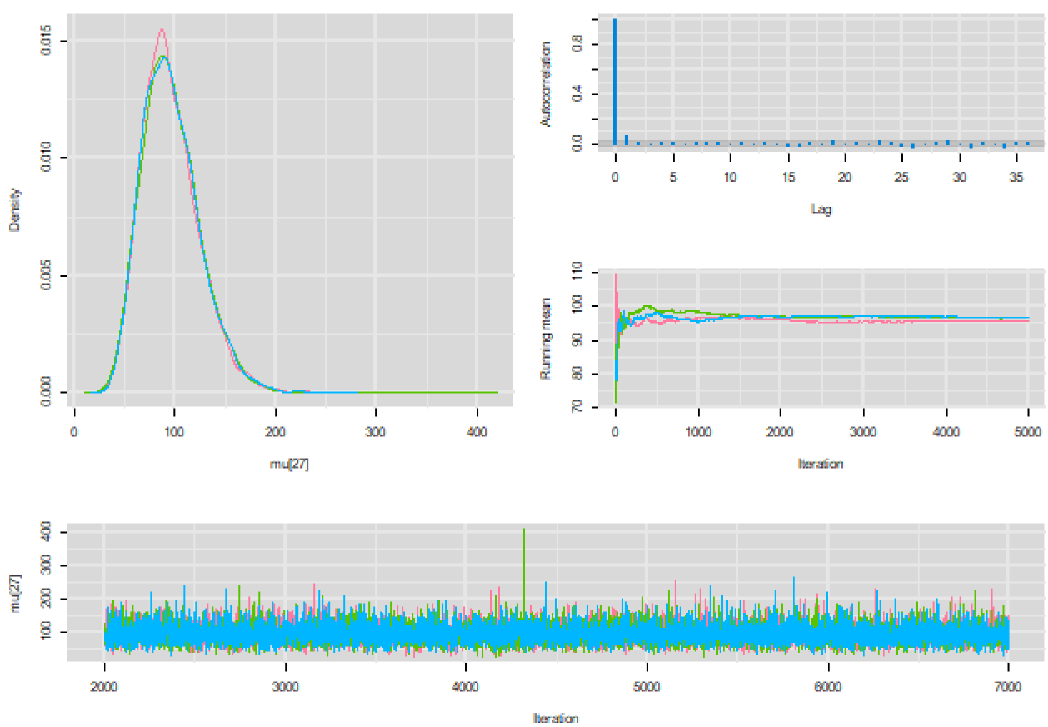

Diagnostics for mu[28]

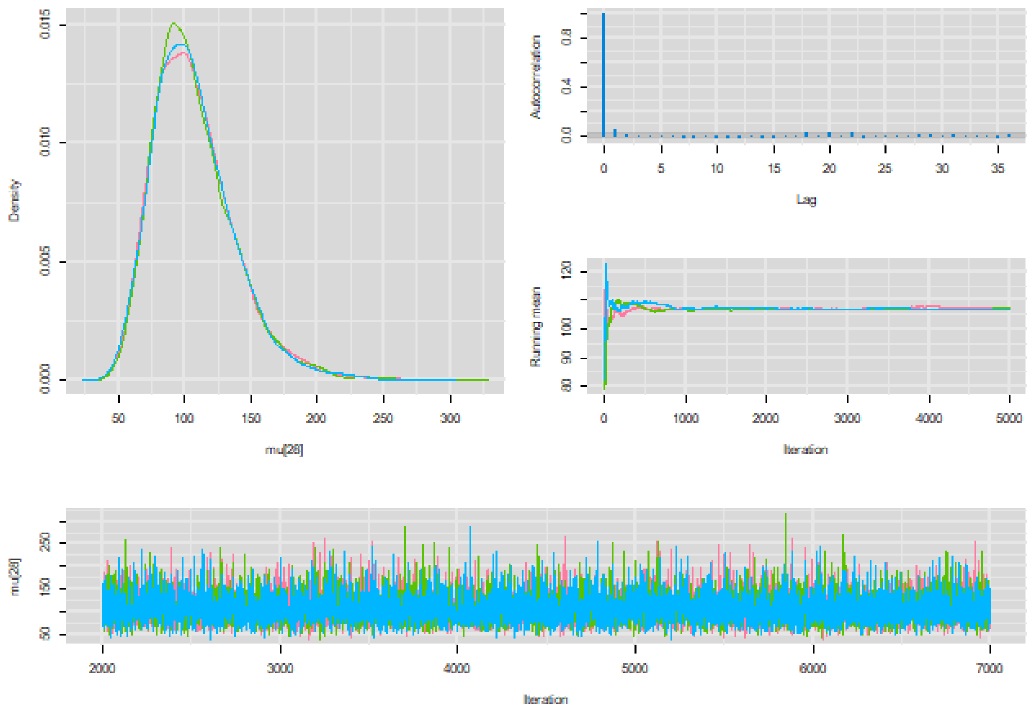

Diagnostics for mu[29]

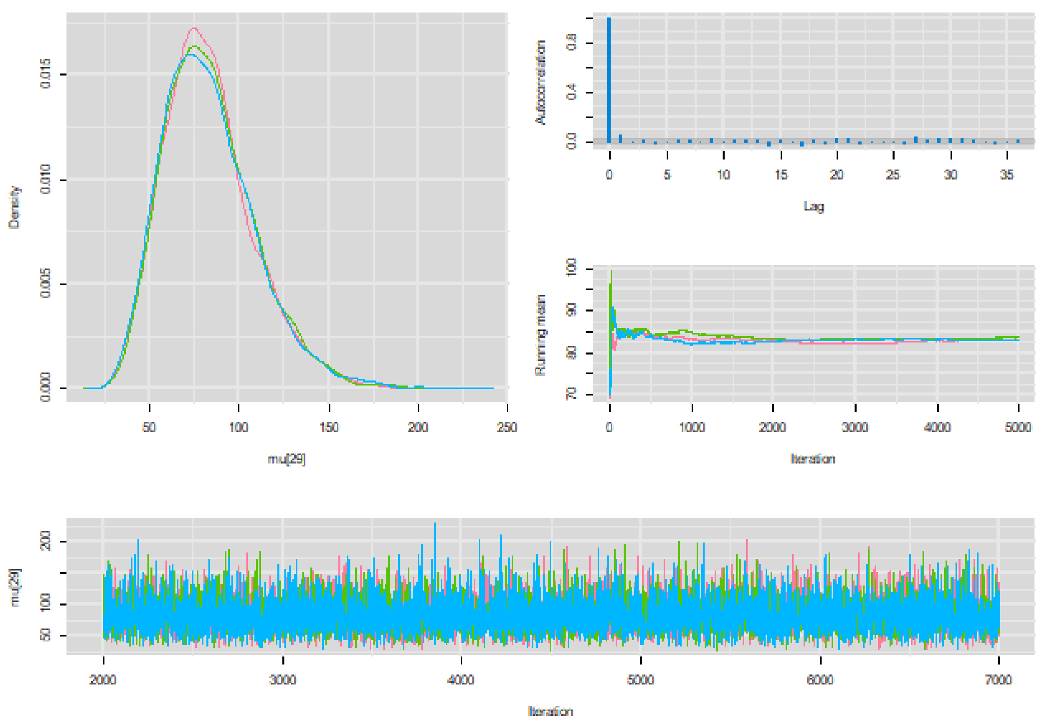

Diagnostics for mu[30]

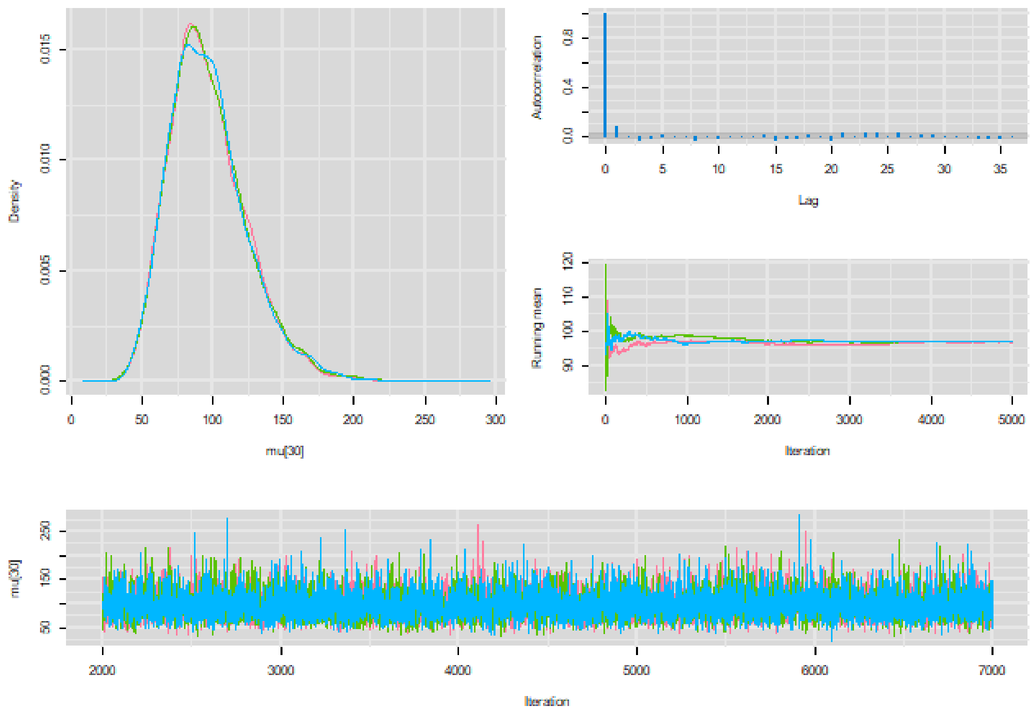

Diagnostics for mu[31]

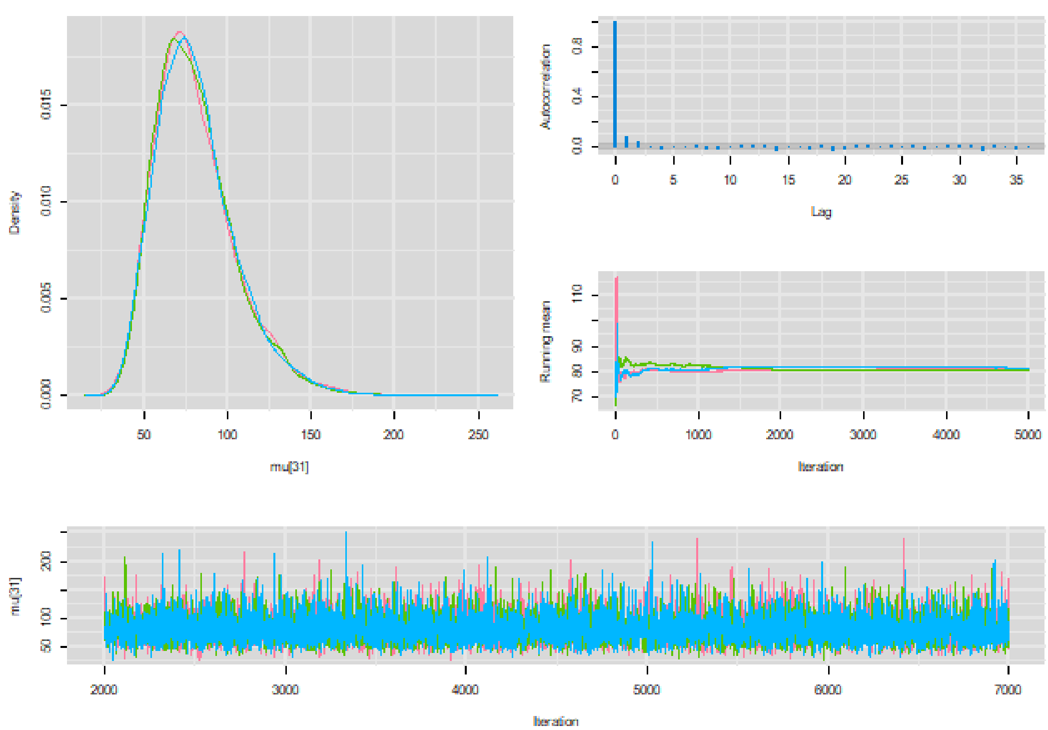

Diagnostics for mu[32]

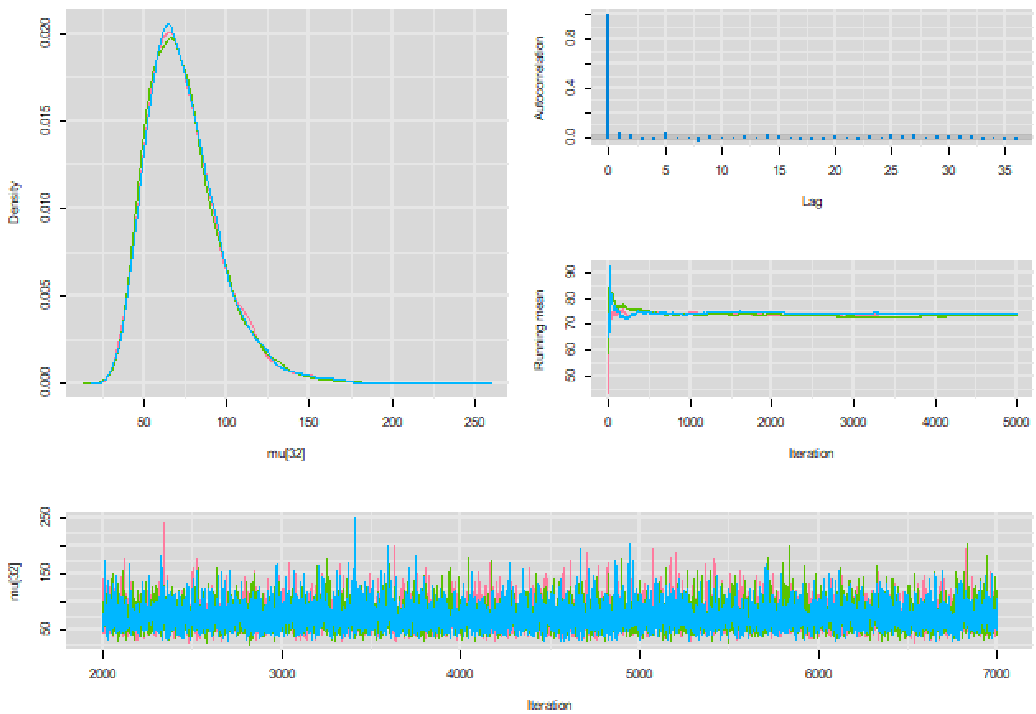

Diagnostics for mu[33]

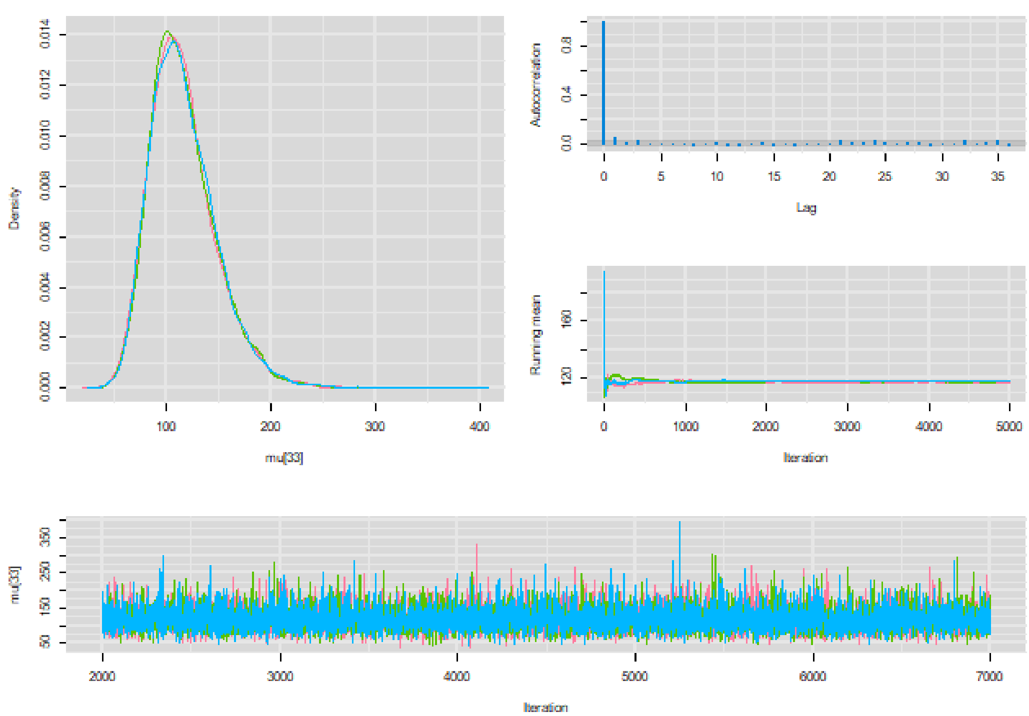

Diagnostics for mu[34]

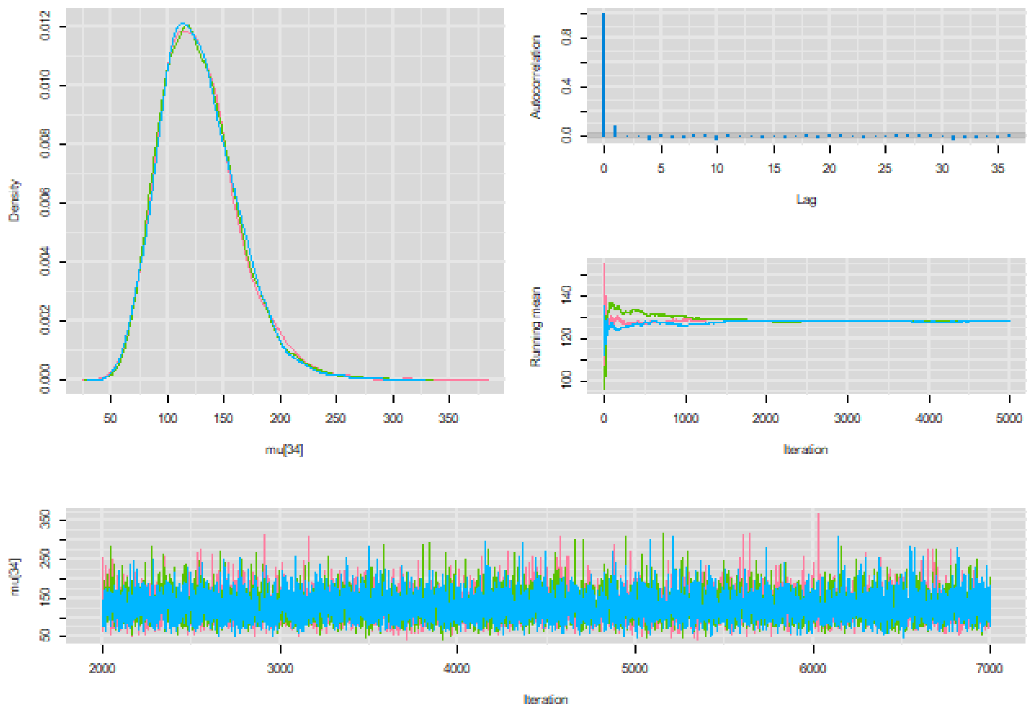

Diagnostics for mu[35]

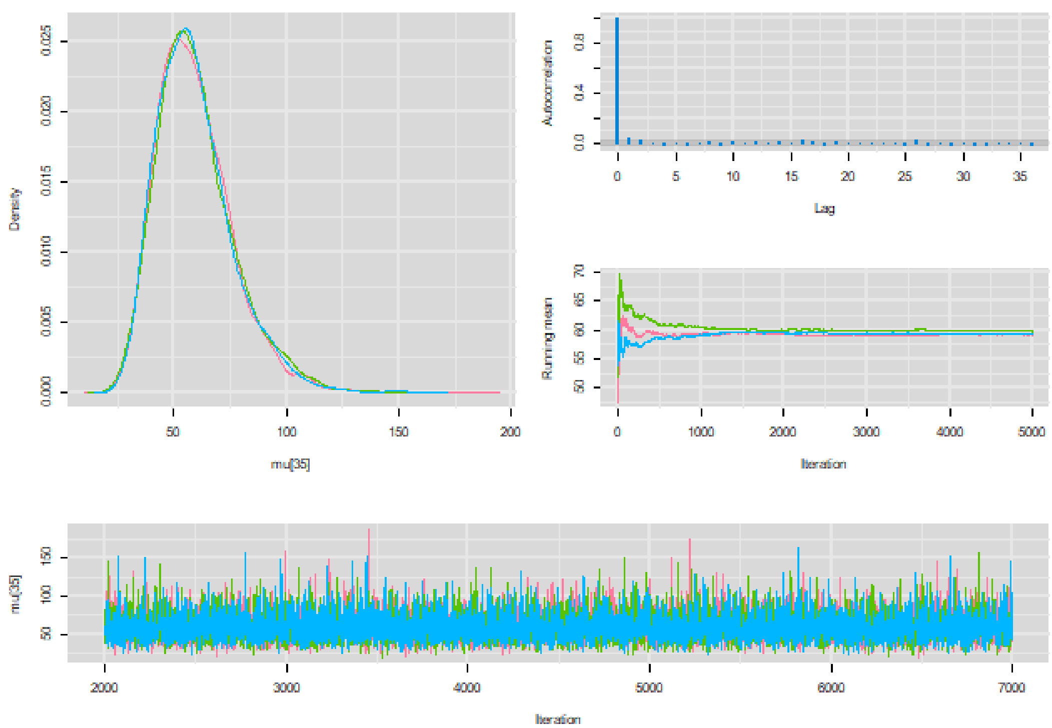

Diagnostics for mu[36]

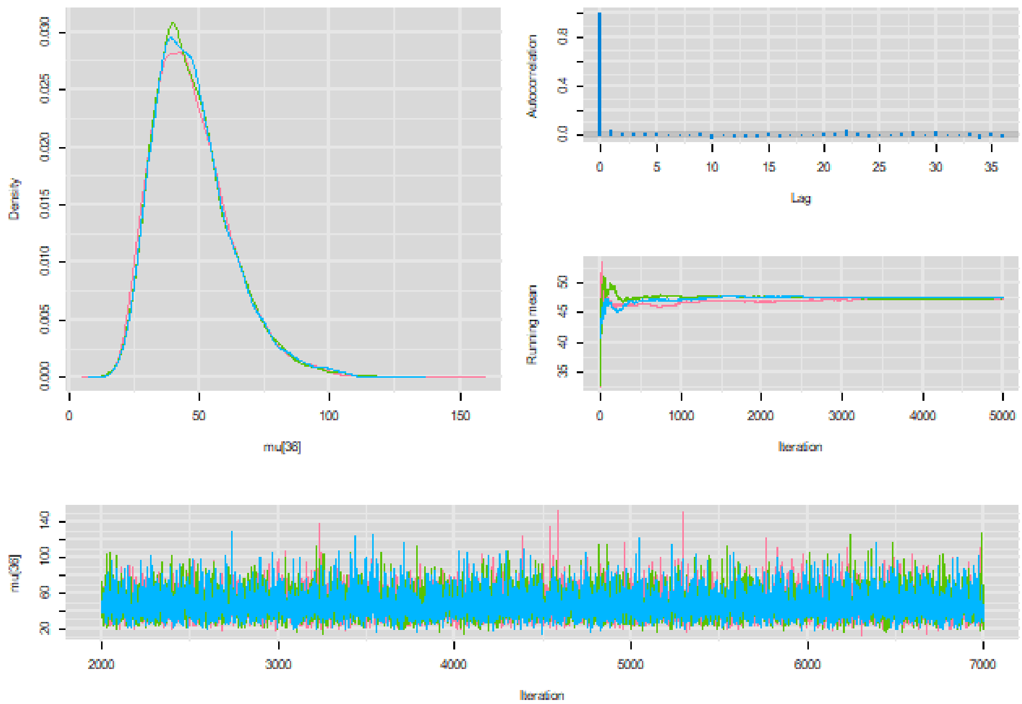

Diagnostics for mu[37]

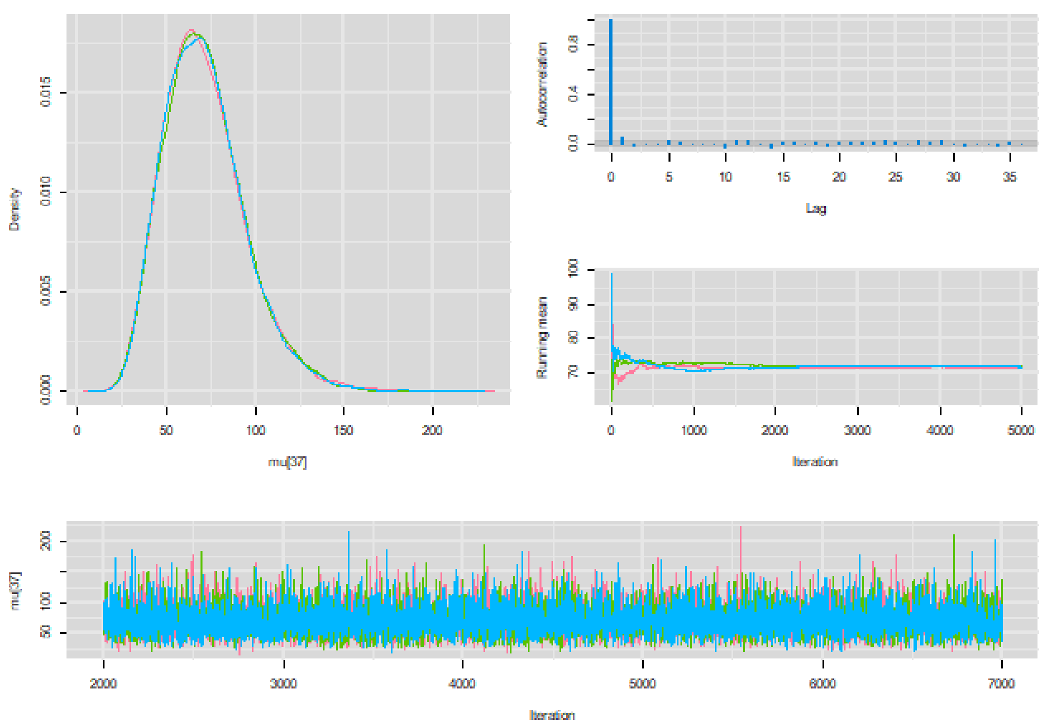

Diagnostics for mu[38]

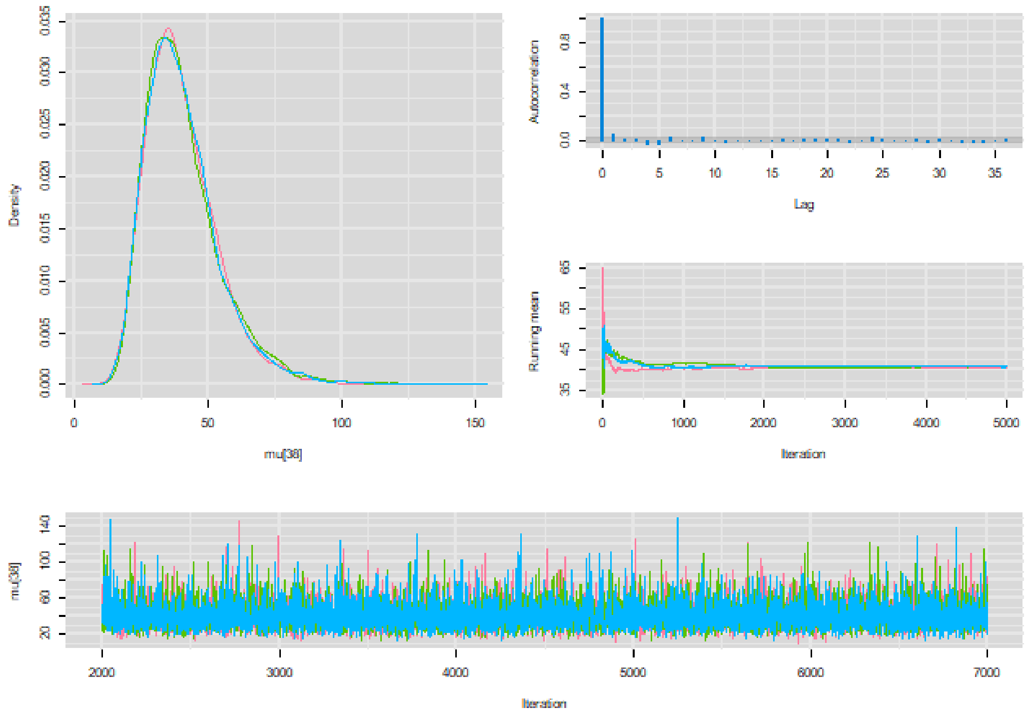

Diagnostics for mu[39]

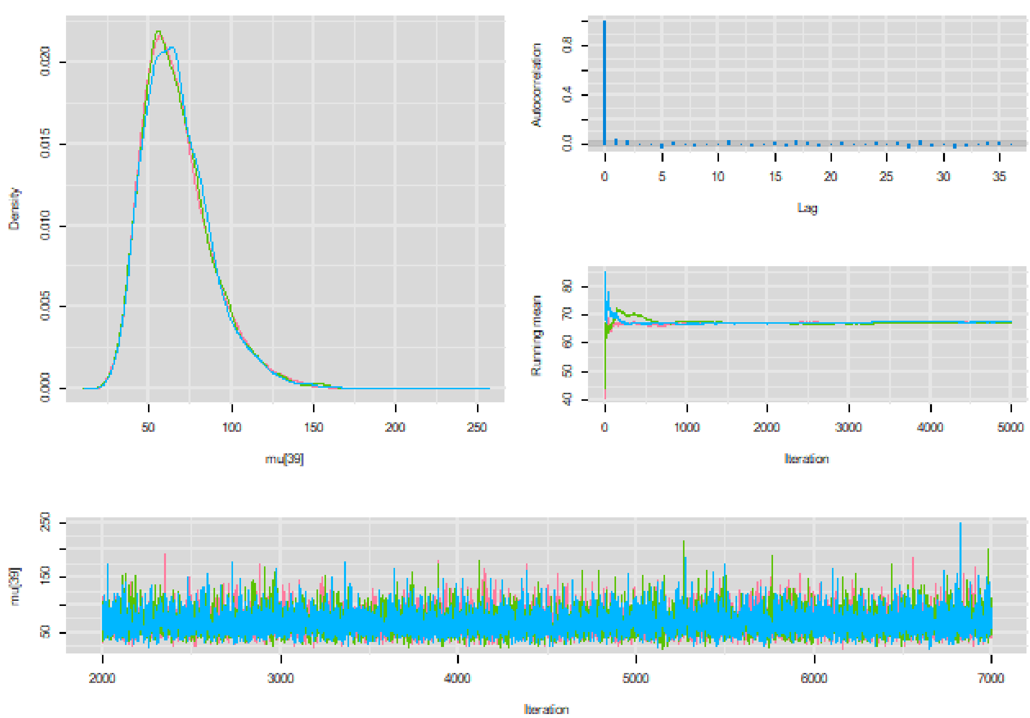

Diagnostics for mu[40]

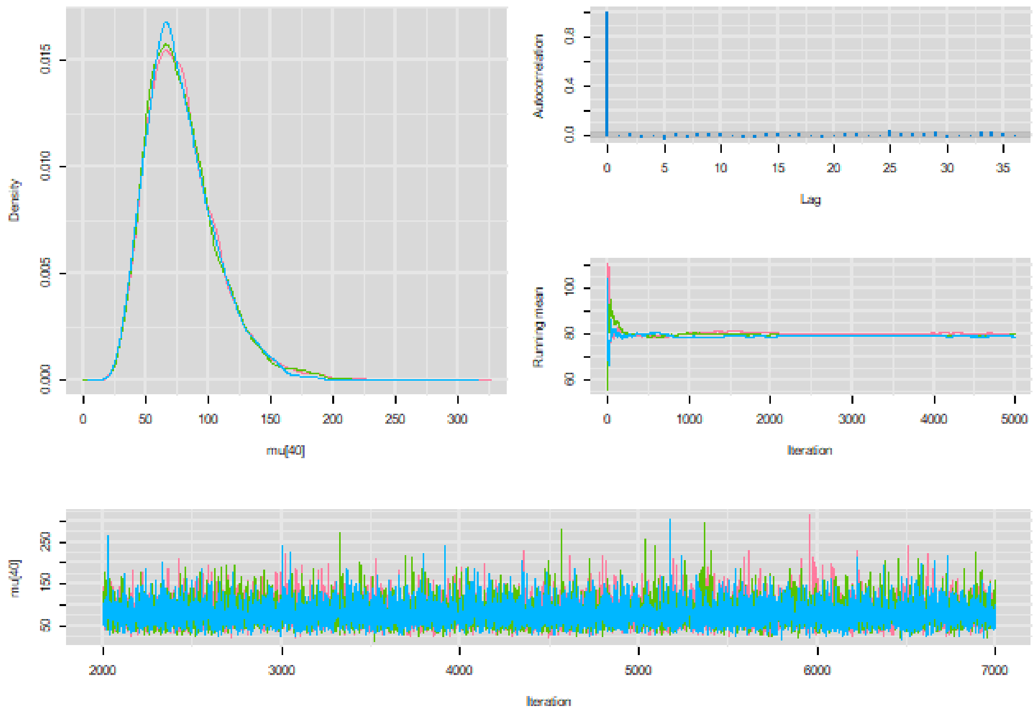

Diagnostics for mu[41]

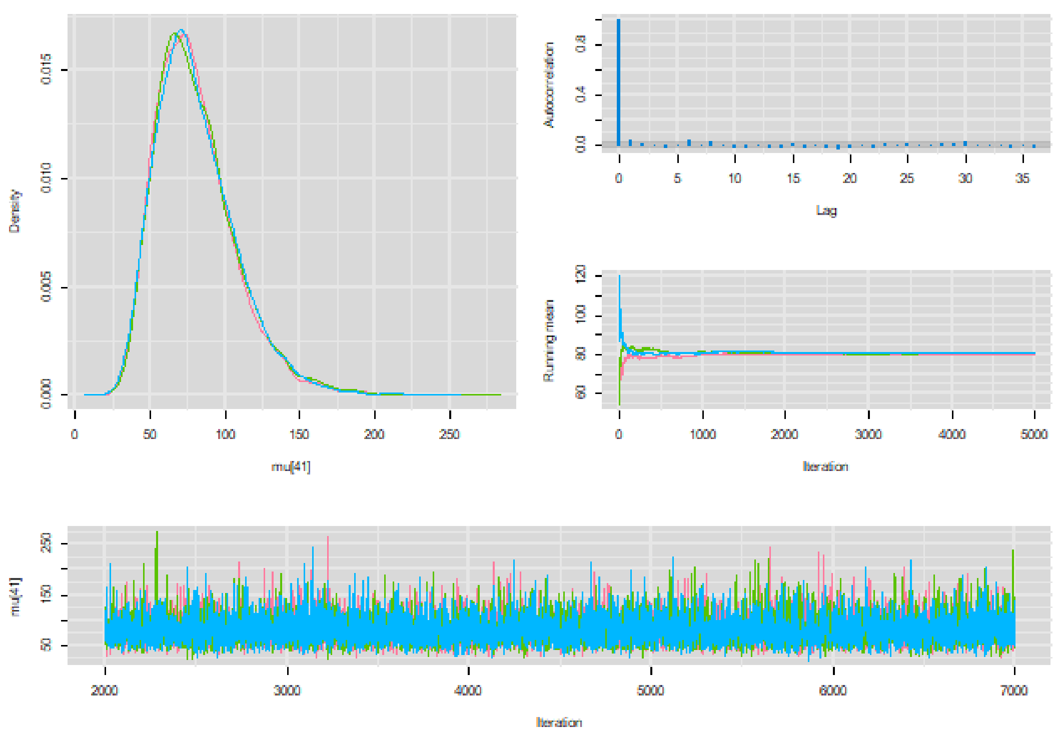

Diagnostics for sigma[1]

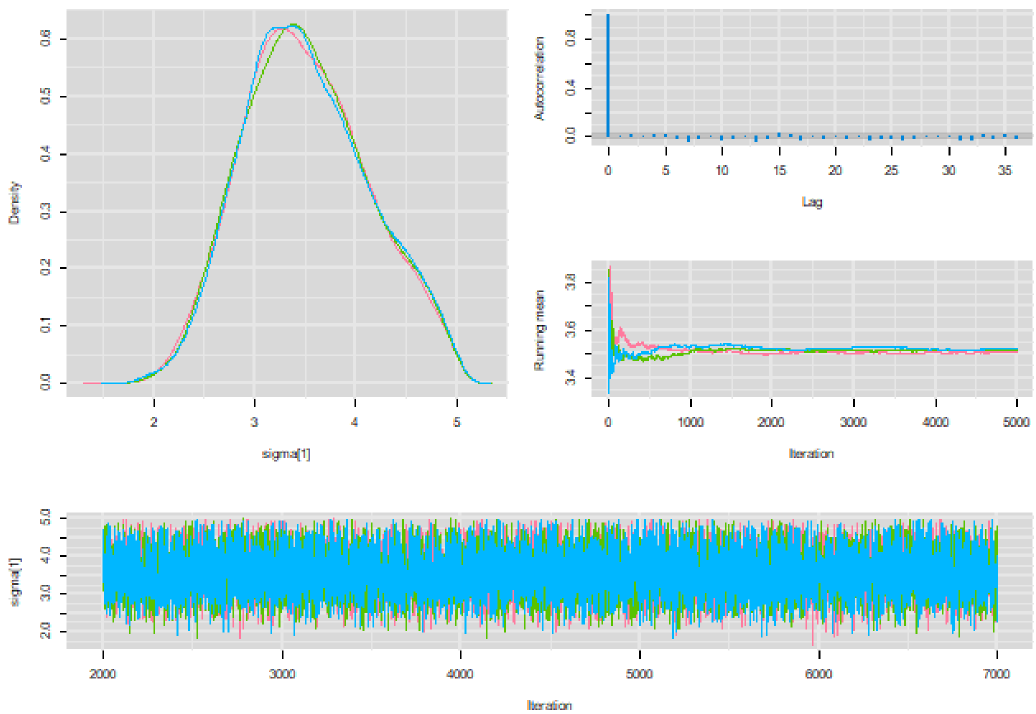

Diagnostics for sigma[2]

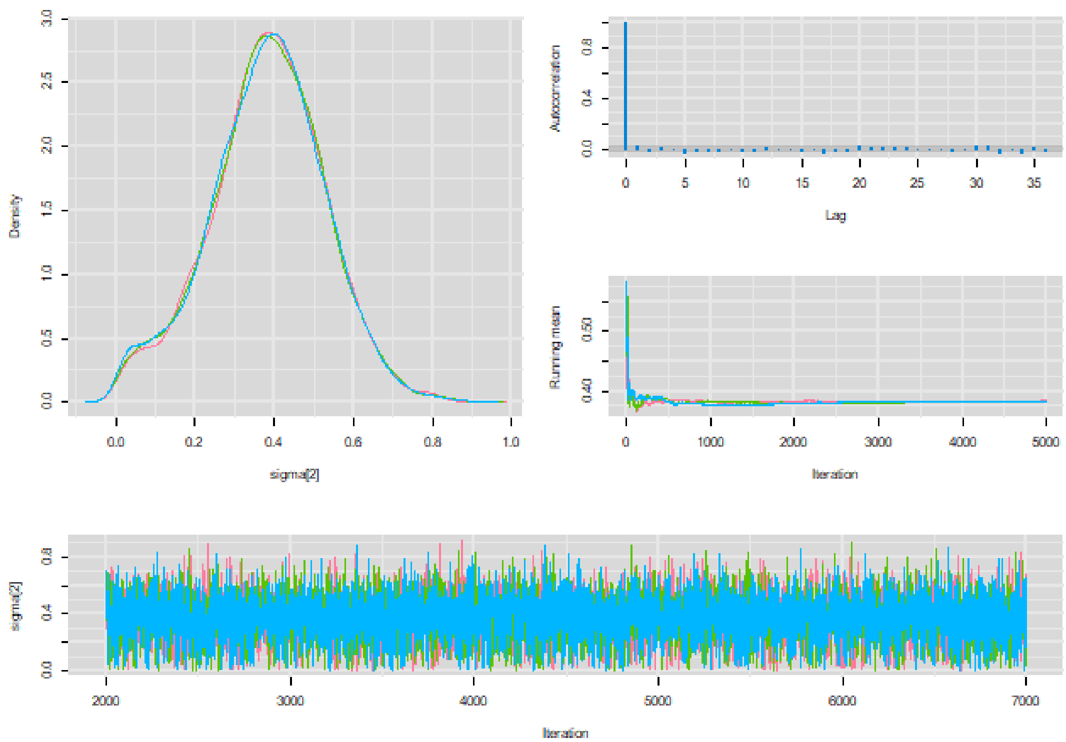

Diagnostics for sigma[3]

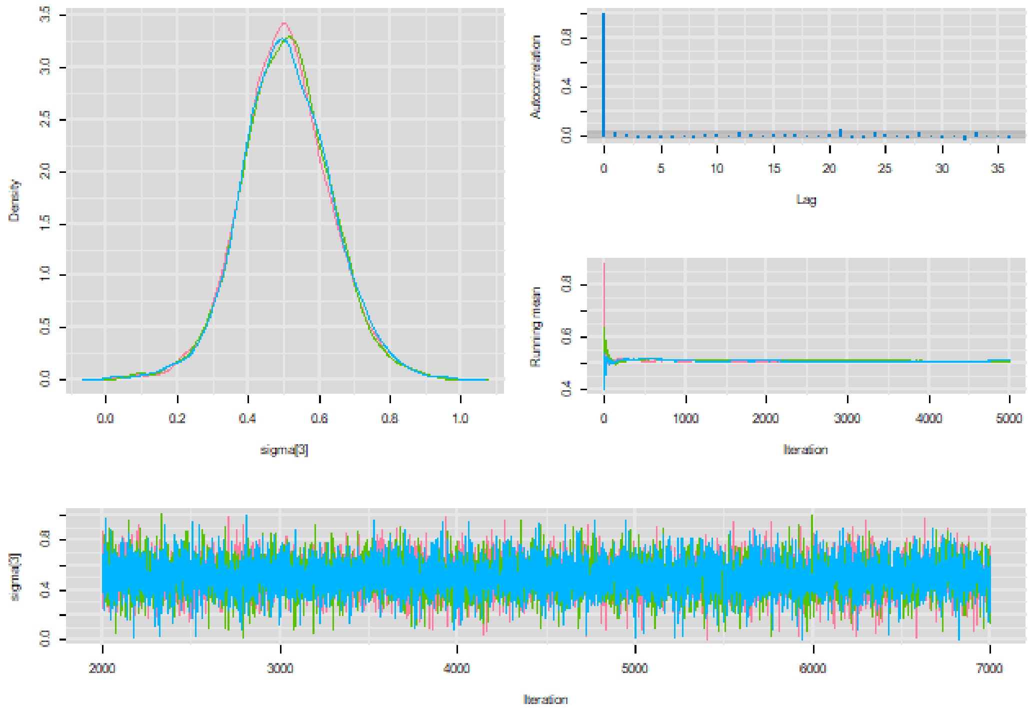

Diagnostics for sigma[4]

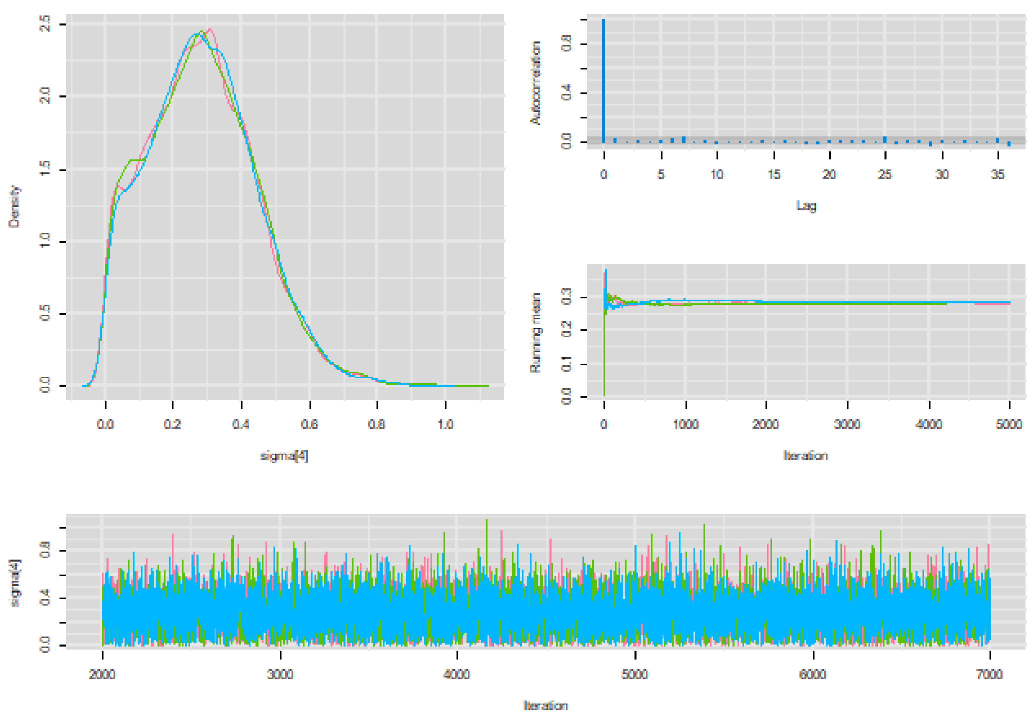

Diagnostics for sigma[5]

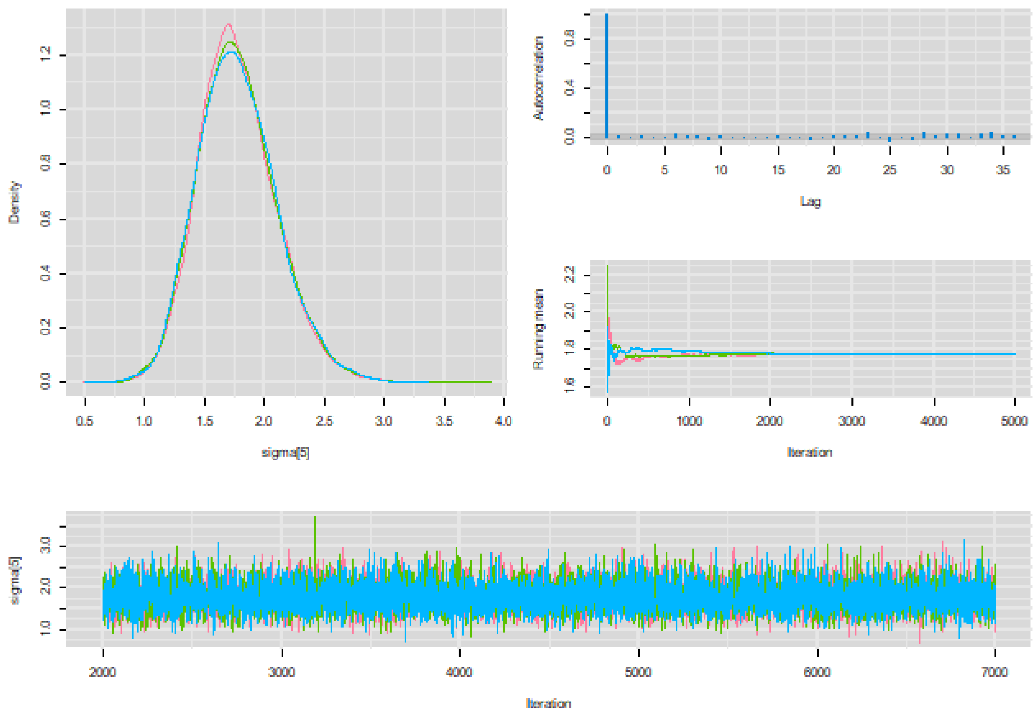

Diagnostics for sigma[6]